# Cargo Routing and Disadvantaged Communities

September 2021

A Research Report from the Pacific Southwest Region University Transportation Center


Miguel Jaller, Associate Professor[1,2,3,4]

Anmol Pahwa, Ph.D. Student[1,2,3,4]

Michael Zhang, Professor[1,3,4]

[1]*Institute of Transportation Studies*
[2]*Sustainable Freight Research Center*
[3]*Department of Civil and Environmental Engineering*
[4]*University of California, Davis*


Pacific Southwest Region UTC
University Transportation Center

ITS UCDAVIS
INSTITUTE OF TRANSPORTATION STUDIES

# TECHNICAL REPORT DOCUMENTATION PAGE

| | | |
|---|---|---|
| **1. Report No.**<br>PSR-UCD-19-43 | **2. Government Accession No.**<br>N/A | **3. Recipient's Catalog No.**<br>N/A |
| **4. Title and Subtitle**<br>Cargo Routing and Disadvantaged Communities | | **5. Report Date**<br>September 2021<br>**6. Performing Organization Code**<br>N/A |
| **7. Author(s)**<br>Miguel Jaller, Ph.D., https://orcid.org/0000-0003-4053-750X<br>Anmol Pahwa, https://orcid.org/0000-0002-9431-3168<br>Michael Zhang, Ph.D., https://orcid.org/0000-0002-4647-3888 | | **8. Performing Organization Report No.**<br>UCD-ITS-RR-21-21 |
| **9. Performing Organization Name and Address**<br>University of California, Davis<br>Institute of Transportation Studies<br>1605 Tilia Street, Suite 100<br>Davis, CA 95616 | | **10. Work Unit No.**<br>N/A<br>**11. Contract or Grant No.**<br>USDOT Grant 69A3551747109 |
| **12. Sponsoring Agency Name and Address**<br>U.S. Department of Transportation<br>Office of the Assistant Secretary for Research and Technology<br>1200 New Jersey Avenue, SE, Washington, DC 20590 | | **13. Type of Report and Period Covered**<br>Final Report (January 2020 – March 2021)<br>**14. Sponsoring Agency Code**<br>USDOT OST-R |
| **15. Supplementary Notes**<br>DOI: https://doi.org/10.7922/G28050WB<br>Dataset DOI: https://doi.org/10.25338/B8934T | | |

**16. Abstract**

Freight is fundamental to economic growth, however, the trucks that haul this freight are pollution intensive, emitting criteria pollutants and greenhouse gases at high rates. The increasing volume and time-sensitivity of freight demand over the past decade has encouraged carriers to take the fastest route, which is often not an eco-friendly route. The increase in urban freight movement has thus brought along negative externalities such as congestion, emissions, and noise into cities. Alternative fuel technologies, such as electric trucks and hydrogen-fuel trucks can significantly reduce freight-related emissions. However, despite their lower operational costs, the high purchase cost and consequent longer payback periods compared to traditional vehicles, have resulted in slow adoption rates. Since the need to reduce global greenhouse gas emissions and local criteria pollutants is immediate, accounting for externalities in carriers' tactical and operational decision-making in the form of eco-routing can bring about desired reductions in emissions. The objectives of this work are to explore the possibilities and potential of eco-routing from the perspective of the carrier, in terms of cost-benefits and trade-offs, and from the perspective of the regulator, in terms of network-wide effects and policy initiatives that could encourage carriers to eco-route. This study evaluates reduction in global greenhouse emissions and local criteria pollutants, with a particular focus on direct impacts on disadvantaged communities in the Southern California Association of Governments (SCAG) region.

| | | | |
|---|---|---|---|
| **17. Key Words**<br>Eco-routing, multi-criteria traffic assignment, origin-based traffic assignment, TAPAS, geofencing | **18. Distribution Statement**<br>No restrictions. | | |
| **19. Security Classif. (of this report)**<br>Unclassified | **20. Security Classif. (of this page)**<br>Unclassified | **21. No. of Pages**<br>55 | **22. Price**<br>N/A |

Form DOT F 1700.7 (8-72) Reproduction of completed page authorized

[page intentionally left blank]

# TABLE OF CONTENTS

## List of Tables

## List of Figures

# About the Pacific Southwest Region University Transportation Center

The Pacific Southwest Region University Transportation Center (UTC) is the Region 9 University Transportation Center funded under the US Department of Transportation's University Transportation Centers Program. Established in 2016, the Pacific Southwest Region UTC (PSR) is led by the University of Southern California and includes seven partners: Long Beach State University; University of California, Davis; University of California, Irvine; University of California, Los Angeles; University of Hawaii; Northern Arizona University; and Pima Community College.

The Pacific Southwest Region UTC conducts an integrated, multidisciplinary program of research, education, and technology transfer aimed at *improving the mobility of people and goods throughout the region*. Our program is organized around four themes: 1) technology to address transportation problems and improve mobility; 2) improving mobility for vulnerable populations; 3) improving resilience and protecting the environment; and 4) managing mobility in high growth areas.

## Disclaimer

The contents of this report reflect the views of the authors, who are responsible for the facts and the accuracy of the information presented herein. This document is disseminated under the sponsorship of the United States Department of Transportation's University Transportation Centers program, in the interest of information exchange. The U.S. Government and the State of California assumes no liability for the contents or use thereof. Nor does the content necessarily reflect the official views or policies of the U.S. Government and the State of California. This report does not constitute a standard, specification, or regulation. This report does not constitute an endorsement by the California Department of Transportation (Caltrans) of any product described herein.

## Disclosure

Dr. Miguel Jaller, Anmol Pahwa, and Dr. Michael Zhang conducted this research titled, “Cargo Routing and Disadvantaged Communities,” at the University of California, Davis, Institute of Transportation Studies. The research took place from January 2020 to March 2021 and was funded by a grant from the U.S. Department of Transportation in the amount of $114,916.00. The research was conducted as part of the Pacific Southwest Region University Transportation Center research program.

## Acknowledgements

This study was funded by a grant from the Pacific Southwest Region (PSR) University Transportation Center and the California Department of Transportation (Caltrans). The authors would like to thank the PSR, USDOT, and Caltrans for their support of university-based research in transportation, and especially for the funding provided in support of this project.

## Abstract

Freight is fundamental to economic growth, however, the trucks that haul this freight are pollution intensive, emitting criteria pollutants and greenhouse gases at high rates. The increasing volume and time-sensitivity of freight demand over the past decade has encouraged carriers to take the fastest route, which is often not an eco-friendly route. The increase in urban freight movement has thus brought along negative externalities such as congestion, emissions, and noise into cities. Alternative fuel technologies, such as electric trucks and hydrogen-fuel trucks can significantly reduce freight-related emissions. However, despite their lower operational costs, the high purchase cost and consequent longer payback periods compared to traditional vehicles, have resulted in slow adoption rates. Since the need to reduce global greenhouse gas emissions and local criteria pollutants is immediate, accounting for externalities in carriers' tactical and operational decision-making in the form of eco-routing can bring about desired reductions in emissions. The objectives of this work are to explore the possibilities and potential of eco-routing from the perspective of the carrier, in terms of cost-benefits and trade-offs, and from the perspective of the regulator, in terms of network-wide effects and policy initiatives that could encourage carriers to eco-route. This study evaluates reduction in global greenhouse emissions and local criteria pollutants, with a particular focus on direct impacts on disadvantaged communities in the Southern California Association of Governments (SCAG) region.

# Cargo Routing and Disadvantaged Communities

## Executive Summary

Can eco-routing be an important step towards sustainable zero-emission transportation? What is the cost-benefit tradeoff for a carrier accounting for emissions in its routing decision (eco-routing)? Generally, the carrier's increased operational costs tradeoff with reduction in emissions from eco-routing, highlighting the lack of incentive for the carrier to eco-route. This result shouldn't be surprising. Had there been a monetary advantage for the carrier to reduce emissions, carriers would consistently eco-route. Moreover, this work found a net monetary loss for the system (private carrier+ society), as the monetary gain from a carrier eco-routing its fleet in the form of reduced emissions for society were offset by the monetary loss for the carrier in the form of increased costs of hauling. Were the benefits from $NO_x$ and $CO_2$ reduction at least 10 times more valuable to society, eco-routing could render a net gain for the system. Yet, it is possible that carriers could choose to eco-route, despite an increase in costs, as this work found that other important travel metrics relevant to the carrier such as travel distance, travel time, and fuel consumed, may reduce due to eco-routing.

To further establish the potential of eco-routing, this study developed the network-wide effects of eco-routing by developing a multi-class improved Traffic Assignment by Paired Alternative Segments (m-iTAPAS) algorithm. With all of the trucks eco-routed in the network, the emission reductions peaked in the range of 1%-5%, at lower congestion levels. This highlights the potential of eco-routing to reduce emissions during off-peak hours, i.e., early morning and late night, when passenger car traffic is significantly lower. Yet it is important to note that while emissions may reduce on aggregate, certain parts of the region may observe a significant rise in emissions. However, such spatial variations in the emissions did not disproportionately affect, either negatively or positively, disadvantaged communities in the SCAG region.

Given the lack of incentive for carriers to eco-route, and the possibility of increased emissions for certain disadvantaged communities, this work explores geofencing as a tool to protect disadvantaged communities in the region. Today, these communities experienced an increased burden. The authors developed two geofences for this work, one for census tracts with high CalEnviroScreen (CES) scores - a pollution exposure index accounting for pollution burden and population characteristics, and another for the Southeast LA (SELA) region. In both cases, emissions within the geofence reduced significantly. $NO_x$ emissions reduced by as much as 70%, due to reduced truck travel within the geofence, although the geofence area may also experience increased passenger car traffic. Again, these reduction in emissions for the geofence area brings along increases in emissions elsewhere in the region. These impacts, though, do not disproportionally affect, either positively or negatively, other disadvantaged communities in the region. Thus, geofencing can bring about a desired outcome in the form of a reduction in emissions for the disadvantaged region, with minimal but equitable increases in network-wide emissions.

# I. Introduction

In the past century, global climate change has become one of the pressing concerns for subsistence of humankind on earth. Swedish scientist, Svante Arrhenius, in 1896 was the first to establish an anthropological link to the rise in global temperatures (Weart, 2008). Ever since then, rigorous scientific evidence has corroborated the greenhouse gas (GHG) effect. Transportation is one of the major sectors that contributes to this effect, amounting to a share of 24% at the global stage, and 34% in the US, for carbon-dioxide ($CO_2$) emissions (Environmental Protection Agency (EPA), 2019a; Tiseo, 2020). Freight movement, which is typically a high-intensity long-duration travel, renders a major chunk of these transportation-related emissions. In 2017, the transportation sector in the US produced 1787 million metric tons of $CO_2$ emissions, about a quarter of which were produced by medium- and heavy-duty trucks alone (Environmental Protection Agency (EPA), 2020). Moreover, of these 1787 million metric tons of $CO_2$ emissions, California produced 218 million metric tons, the second highest for any state in the US, behind only Texas (Environmental Protection Agency (EPA), 2019b).

Beyond freight's impact on global climate change, criteria pollutants from urban freight movement adversely affect the health of local populations. The recent trends in freight distribution with the growth of e-commerce and subsequent rise of rush-deliveries has significantly affected urban freight flows, resulting in frequent less-than-truckload urban freight movement on faster routes which often are not energy-efficient or eco-friendly (Jaller et al., 2020b). Such urban freight movement thus brings negative externalities such as congestion, noise and air pollution (Jaller and Pahwa, 2020), which particularly affect disadvantaged communities, where logistic facilities may be concentrated owing to lower property rates. Jaller and Pineda (2017), Jaller et al. (2020a), and Jaller et al. (2020b) evinced this logistics relocation and freight concentration in the core, dense, urban parts of Southern California. Such logistics relocation closer to the urban core, however, also provides opportunities for the use of zero-emission vehicles in the last-mile distribution. Thus, to foster a sustainable and eco-friendly freight movement, the state incentivizes carriers to transition towards Zero-Emission Vehicles (ZEVs) with the California Sustainable Freight Action plan, Air Resources Board regulations for zero emission trucks and the Advanced Clean Truck (ACT) rule. However, a significant change in the carrier's fleet can take a considerable amount of time, while there is an urgent need for operational improvement initiatives that could provide efficient alternatives to address global climate change and local pollution impacts of urban freight in Southern California. Towards this end, policy initiatives that encourage and incentivize carriers to account for emissions in their routing decisions (eco-friendly truck routing) could make more immediate contributions to solving the imminent environmental crisis.

The objective of this work is to explore possibilities related to eco-friendly routing for the carriers and regulators in the Southern California Association of Governments (SCAG) region. To do so, the authors will explore the potential of eco-routing from: 1) the perspective of the carrier, in terms of cost-benefits and trade-offs for a carrier eco-routing in a stochastic network; and 2) the perspective of the system (e.g., regulator, society) in terms of 2.1) network-wide reductions in emissions from system-wide truck eco-routing, and 2.2) policy initiatives such as

geofencing, access control, and infrastructure use restrictions that could mitigate negative impacts of urban freight movement for disadvantaged communities.

The following section (Section 2) discusses pertinent literature pertaining to eco-routing, vehicle routing and traffic assignment. Section 3 presents the workflow and the methodology for this study. Section 4 and 5 then develop the numerical experiments and the results for the case study of SCAG. This study concludes with a discussion of the results (Section 5), particularly in the context of possible immediate policy initiatives that would serve as an intermediary step towards the long-term objective of freight sustainability.

# II. Literature Review

With a growing pressure for sustainable transportation, the last couple of decades have witnessed a substantial increase in studies related to eco-routing. In the context of the scope of analysis, these studies largely pertain to point-to-point routing (Huang and Peng, 2018; Schröder and Cabral, 2019), classical vehicle-routing problem (VRP) (Erdoğan and Miller-Hooks, 2012; Hooshmand and MirHassani, 2019) or traffic assignment (Ahn and Rakha, 2008; Guo et al., 2012). In order to evaluate fuel consumption and emissions, some of the earlier work (Ericsson et al., 2006) relied on single point values (macroscale models), while more recent work have employed mesoscale (Yao and Song, 2013) and microscale (Nie and Li, 2013) models, accounting for different factors that can influence vehicle efficiency. Zhou et al. (2016) broadly categorized these factors into travel, weather, vehicle, roadway, traffic, and driver related. Research work with in-situ and in-vitro experiments estimated the impacts of these factors on vehicle efficacy and thus developed meso and microscale models (Huang et al., 2018).

Mesoscale models estimate fuel consumption and emission rates from aggregated information, such as average vehicle speed on the street, average street grade, etc., while more sophisticated microscale models employ traffic dynamics and vehicle trajectories for more precise estimates. Literature has commonly categorized these models as white-box, e.g., carbon balance; grey-box; and black-box models, e.g., VTMicro, CMEM, EMFAC; in the order of most to least transparent between inputs and output. In practice, the impacts of the aforementioned factors are realized by strategic, tactical, and operational decision-making (Sivak and Schoettle, 2012). In the context of routing, these strategic decisions are long-term decisions related to the vehicle type and configuration, tactical decisions on the other hand pertain to route choice and amount of payload, while the operational decisions account for driving style. While the decision to eco-route involves an obvious trade-off between travel time/travel distance and fuel consumption/emissions, eco-friendly paths may also render savings in cost (Yao and Song, 2013; Zeng et al., 2016). Figure 1 provides a taxonomy of the eco-routing literature, and Table 1 presents a non-exhaustive list of different eco-routing studies, summarizing the transportation problem addressed, and the externalities considered in the study.

In general, fuel consumption and emission models are convex shaped curves that achieve peak efficiency at moderate levels of vehicle operation, i.e., speed, acceleration, and braking. Passiveness or aggression on the pedal renders a drop in vehicle efficiency, increasing overall fuel consumption and vehicle emissions. Hence, eco-routing encompasses a trade-off between trip travel distance/time and vehicle efficiency (emissions and fuel consumption), which may also result in cost savings. Ericsson et al. (2006) for instance, found that about half of all the trips in the city of Lund, Sweden did not take the most fuel-efficient path, and could reduce fuel consumption by about 8% if they did so. Yao and Song (2013) identified that mid-range distance trips (5-10mi) under heavy congestion can have a significant reduction in fuel consumption, though at the cost of a substantial increment in travel time in comparison to the fastest path.

**Figure 1. Taxonomy of eco-routing literature**

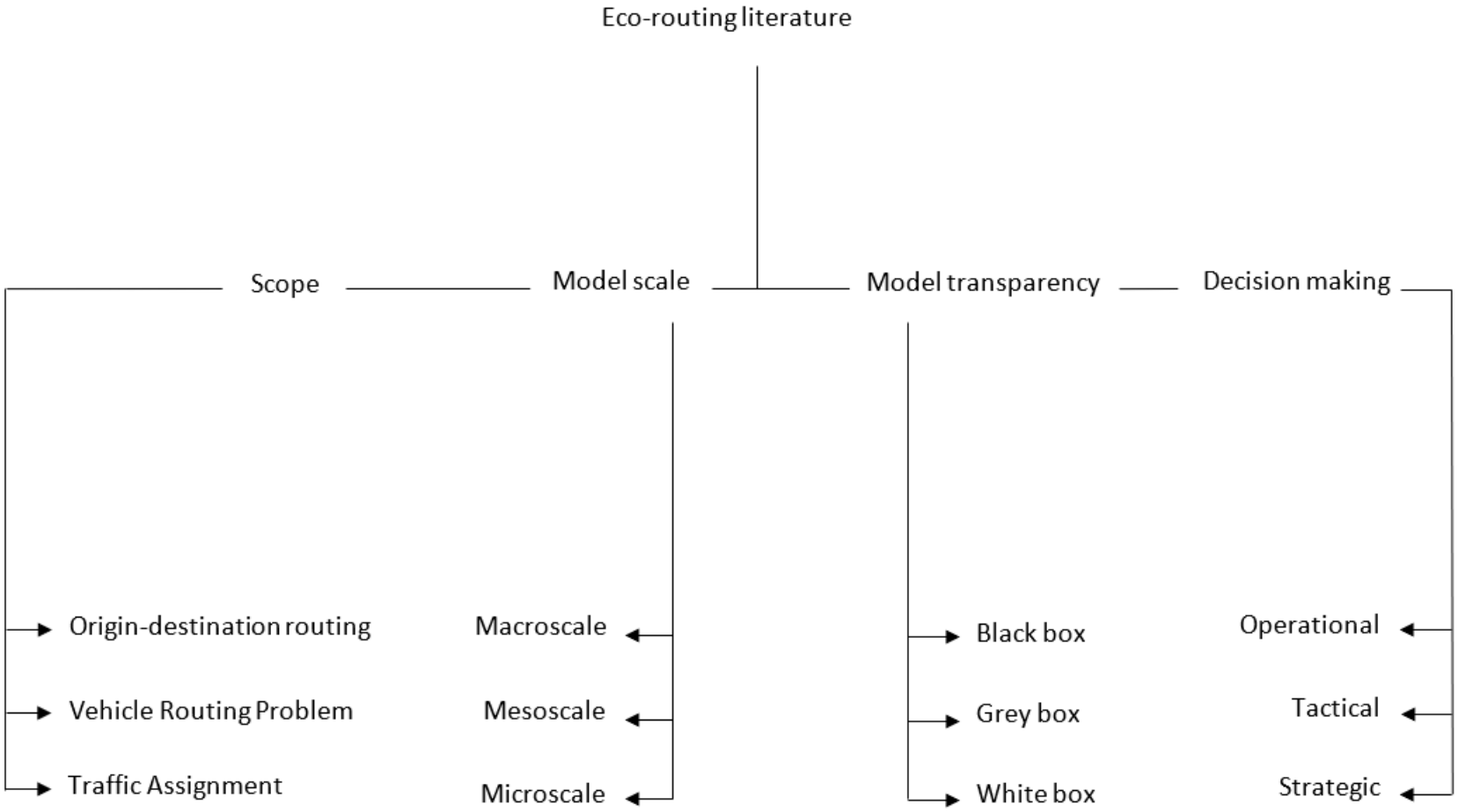


This study performs eco-routing analyses in the context of origin-destination routing and traffic assignment, using mesoscale black box models, thus incorporating emissions in carrier's tactical and operational decision making.

**Table 1. A non-exhaustive summary of eco-routing studies**

| Research article | Scope | Key Feature | Externality considered |
|---|---|---|---|
| Ericsson et al. (2006) | PPR | Streel level FC modeling | FC |
| Nie and Li (2013) | PPR | Microscopic FC modeling | FC, $CO_2$ |
| Yao and Song (2013) | PPR | Time-dependent model | FC, $CO_2$ |
| Bandeira et al. (2014) | PPR | Strategic decision making | FC, CO, $CO_2$, HC, $NO_x$ |
| Scora et al. (2015) | PPR | Freight specific eco-routing | FC |
| Sun and Liu (2015) | PPR | Microscopic FC modeling | FC, CO, $CO_2$, HC, $NO_x$ |
| Zeng et al. (2016) | PPR | Multi-objective routing | FC, $CO_2$ |
| Huang and Peng (2018) | PPR | Emission constrained routing | FC |
| Schröder and Cabral (2019) | PPR | 3-dimensional routing model | FC |
| Tzeng and Chen (1993) | TA | Multi-objective modeling | CO |
| Rilett and Benedek (1994) | TA | System equitable assignment | CO |
| Benedek and Rilett (1998) | TA | System equitable assignment | CO |
| Nagurney et al. (1998) | TA | Pollution permits | Generic |
| Nagurney (2000) | TA | Strategic decision making | Generic |
| Sugawara and Niemeier (2000) | TA | Emission-flow relationship | CO |
| Ahn and Rakha (2008) | PPR, TA | Micro-simulation study | FC, CO, $CO_2$, HC, $NO_x$ |
| Guo et al. (2012) | TA | Multiclass TA | FC, CO, $NO_x$ |
| Rakha et al. (2012) | TA | Multiclass TA | FC, CO, $CO_2$, HC, $NO_x$ |
| Aziz and Ukkusuri (2014) | TA | Time-dependent modeling | $CO_2$ |
| Elbery et al. (2016) | TA | Ant colony-based assignment | FC, CO, $CO_2$, HC, $NO_x$ |
| Elbery and Rakha (2019) | TA | Eco-routing market penetration | FC |
| Figliozzi (2010) | VRP | Time-dependent modeling | $CO_2$ |
| Erdoğan and Miller-Hooks (2012) | VRP | Strategic decision making | FC |
| Hooshmand and MirHassani (2019) | VRP | Time-dependent modeling | FC, $CO_2$ |
| **This work** | PPR, TA | Stochastic routing multiclass TA with geofencing freight specific eco-routing | FC, $CH_4$, $CO_2$, CO, $NO_x$, PM, ROG |

FC – Fuel Consumption, PPR – Point-to-Point Routing, VRP – Vehicle Routing Problem, TA – Traffic Assignment

Similar conclusions were drawn by Zeng et al. (2016). The authors in the study found that the eco-route, the shortest, and the fastest path were in ascending order for emissions and descending order for travel time. Scora et al. (2015) found a 16% reduction in fuel consumption with eco-friendly routing, but much like other studies, the authors also observed a 31% increment in travel time for the same. Yet, about half of all of the eco-friendly routes resulted in a small, on average 2%, reduction in total cost. Other important studies have evaluated the impact of congestion and road grades in the emissions and fuel consumption for eco-routing and eco-driving initiatives (Barth and Boriboonsomsin, 2008, 2009; Boriboonsomsin et al., 2012). In the context of vehicle-routing, Figliozzi (2010) also suggested a possible reduction in emissions with little or no increment in operational cost. While these results are limited to an analysis of certain origin-destination pairs, network-wide effects of eco-routing have also been established previously.

As mentioned, beyond routing, the impacts of eco-routing have also been studied under traffic equilibrium. In this context, Tzeng and Chen (1993) is one of the earliest works, wherein the authors established emissions-based User Equilibrium (UE) for the city of Taipei, Taiwan. While the study found an emissions-based assignment to reduce total pollution by 27%, the total network travel time was up by 14% in comparison to the conventional time-based assignment. Rilett and Benedek (1994) went a step further and compared System Optimal (SO) and User Equilibrium (UE) performance for travel-time based and carbon-monoxide (CO)-based traffic assignment. While the SO-CO assignment had a 3% increment in network travel-time, it far outperformed the UE-CO assignment, which observed a 9% increment in comparison to the system optimal travel time. Later, in Benedek and Rilett (1998), the authors performed an equitable traffic assignment with CO-a societal objective wherein the aim was to have equal CO pollution in major residential corridors. While this resulted in an equal distribution of externalities, the overall pollution levels in the network increased consequently. More recently, Guo et al. (2012) and Elbery and Rakha (2019) evaluated the impact of eco-routing on network penetration, performing a multi-criteria traffic equilibrium. In the latter, the authors developed a targeted network penetration, wherein for any level of network penetration, the vehicles that rendered the highest savings from eco-routing were eco-routed. In process, the network achieved saturation level, i.e., a 12% emission reduction at only 40% penetration, with a 3% increment in network travel time. In comparison, randomized network penetration achieved a similar 12% emission reduction at 90% penetration, but at the cost of a much higher 8% increase in total travel time.

These studies therefore highlight the potential benefits from eco-routing and the need to develop policy initiatives that can encourage eco-friendly routing. As discussed earlier, alternate fuel vehicles such as electric trucks, hydrogen-fuel trucks, etc., can mitigate negative externalities from freight. Yet, despite government efforts to incentivize carrier fleet transition to zero-(tailpipe)-emission vehicles, adoption rates have been slow. Towards this end, eco-friendly truck routing can render reductions in emissions to a lesser but significant extent. Thus, the objectives of this work are to explore the possibilities and potential of eco-routing from the perspective of the carrier, in terms of cost-benefits and trade-offs, and from the perspective of the regulator, in terms of network-wide effects and policy initiatives that could encourage carriers to eco-route. This study evaluates reduction in global greenhouse gas emissions and local criteria pollutants, with a particular focus on direct impacts on disadvantaged communities in the Southern California Association of Governments (SCAG) region. These disadvantaged communities are identified and established using California Communities Environmental Health Screening Tool (CalEnviroScreen; CES) scores, a pollution exposure index accounting for pollution burden and population characteristics (California Office of Environmental Health Hazard Assessment, 2017). This study aligns with California's efforts to further environmental justice which calls for fair treatment of individuals and communities regardless of identity, status, or income (California Environmental Protection Agency, n.d.).

# III. Methodology

To develop a comprehensive understanding of eco-routing, this work explores its potential from the perspective of a carrier hauling truck fleet operating between different origin-destination pairs in the form of expected cost-benefits, trade-offs, and travel reliability from minimizing expected emissions (eco-routing) in a stochastic network with probabilistic arc speeds. Additionally, the authors consider the network-wide effects of truck eco-routing using traffic assignment from a systems perspective, or the perspective of a regulator. This work carries out numerical analyses for the Southern California Association of Governments (SCAG) region, with a particular focus on disadvantaged communities and initiatives that could mitigate negative impacts on disadvantages communities. This work develops: a) a point-to-point routing tool for a stochastic network with (empirically developed) probabilistic arc speeds; and b) a multi-class traffic assignment tool. Fundamental to all of the analyses, the authors develop mesoscale emission and vehicle fuel consumption rate models. Specifically, this study develops the shortest path (SP), fastest path (FP), least-emissions path (LEP), and least-cost path (LCP) truck routing over specific origin-destination pairs and establishes a corresponding multi-class traffic equilibrium to evaluate the network-wide effects of eco-routing. Below are the formulations and solution algorithms for point-to-point truck routing in a stochastic network with probabilistic arc speeds, and multi-class traffic assignment.

## Point-to-point routing in a stochastic network with probabilistic arc speeds

To begin, the authors introduce a network as a directed graph - $G(N, A)$, with a set of nodes $N$ and a set of arcs $A = \{(i,j); i,j \in N\}$. A vehicle traversing through this network observes costs pertaining to travel-related parameters $p \in P$, which manifest on the arc at a rate defined by a polynomial function on arc speed, given by, $\sum_n \eta_n^p v_{ij}^n$, where $\eta_n^p$ is the coefficient of the polynomial term $v_{ij}^n$ (arc speed $v_{ij}$ raised to the power $n$).

$N$: Set of nodes
$A$: Set of arcs
$P$: Set of parameters
$c_{ij}$: Cost of arc $(i,j)$
$d_{ij}$: Length of arc $(i,j)$
$v_{ij}$: Vehicle speed on arc $(i,j)$
$t_{ij}$: Travel time on arc $(i,j)$
$x_{ij}$: Binary: 1 if arc $(i,j) \in A$ is traversed by the vehicle, else 0 $(i,j)$
$\theta_p$ : Cost of parameter $p$
$\eta_n^p$: Coefficient of $v_{ij}^n$ for parameter $p$
$r, s$: Origin, Destination

Thus, the generalized arc cost $c_{ij}$ is,

$$c_{ij} = \sum_{p \in P} \theta_p t_{ij} \sum_n \eta_n^p v_{ij}^n \quad (1)$$

$$t_{ij} = \frac{d_{ij}}{v_{ij}} \quad (2)$$

To develop a comprehensive understanding of eco-routing, this work assumes a stochastic nature of the network with arc speeds being probabilistic. Under such a stochastic setting, the authors assume a priori decision making, with posterior realization of arc costs, rendering the objective function as,

$$\min_{x_{ij};\,(i,j) \in A} z = \sum_{(i,j) \in A} E[c_{ij}] x_{ij} \quad (3)$$

$$v_{ij} \sim f_{v_{ij}} \quad (4)$$

Subject to flow conservation,

$$\sum_{i \in T(j)} x_{ij} = \sum_{k \in H(j)} x_{jk} \quad (5)$$

$$\sum_{j \in H(r)} x_{rj} = 1 \quad (6)$$

$$\sum_{i \in T(s)} x_{is} = 1 \quad (7)$$

Where, $H, T$ are the node predecessor (tail) and successor (head) functions, respectively.

$$T(i) = \{k; (k,i) \in A\} \quad (8)$$

$$H(i) = \{k; (i,k) \in A\} \quad (9)$$

The above-developed optimization is analogous to the deterministic routing problem, and hence can be solved by classical Dijkstra's algorithm (Dijkstra, 1959) .

## Multi-class traffic assignment

For the purpose of traffic assignment analysis, again, the authors define the network as a directed graph - $G(N, A)$, with $N$ and $A$ denoting sets of nodes and arcs in the network, respectively. Further, this section introduces a set of origins $R$ and a set of destination $S$ with demand $q_{rs}$ between origin $r \in R$ and destination $s \in S$. To explore network-wide impacts of truck eco-routing, the authors assume $K$ classes of vehicles in the network, wherein vehicle class $k \in K$ traverses arc $(i,j) \in A$ at cost $c_{ij}^k$, defined on the parameters from the set $P$.

$N$: Set of nodes
$A$: Set of arcs
$P$: Set of parameters
$R$: Set of origins
$S$: Set of destinations
$K$: Set of vehicle classes
$q_{rs}^k$: Demand for vehicle class $k$ between origin $r$ and destination $s$

$S_r$: Set of destinations with non-zero demand from origin $r$ $\{s \in S: q_{rs}^k > 0\}$
$c_{ij}^k$: Cost of arc $(i,j)$ for vehicle class $k$
$d_{ij}$: Length of arc $(i,j)$
$v_{ij}$: Vehicle speed on arc $(i,j)$
$t_{ij}$: Travel time on arc $(i,j)$
$x_{ij}$: Flow on arc $(i,j)$
$x_{ij}^{kr}$: Flow of vehicle class $k$ on arc $(i,j)$ from origin $r$
$V_{ij}$: Volume capacity for arc $(i,j)$
$\alpha_{ij}$: BPR parameters for arc $(i,j)$
$\beta_{ij}$: BPR parameter for arc $(i,j)$
$\theta_p$ : Cost of parameter $p$
$\eta_n^p$: Coefficient of $v_{ij}^n$ for parameter $p$

A vehicle traversing through the network observes costs pertaining to travel-related parameters from the set $P$, which manifest on the arc at a rate defined by the polynomial function on arc speed, given by, $\sum_n \eta_n^p v_{ij}^n$. This generalized cost function, must be strictly positive, continuously differentiable, and monotonically non-decreasing to guarantee the existence of the traffic assignment solution, uniqueness of the equilibrium, and absence of infinite loops, respectively. Additionally, this work assumes arc costs to be separable, i.e., costs on an arc only depend on the flow of that arc and none other. These assumptions are further explained, enforced, and explored in the Appendix - A. Unlike in the previous subsection, the arc travel time here is deterministic, defined by the BPR function.

$$c_{ij}^k(x_{ij}) = \sum_{p \in P} \varphi_p^k \theta_p t_{ij}(x_{ij}) \sum_n \eta_n^p v_{ij}^n \tag{10}$$

$$t_{ij}(x_{ij}) = t_{ij}^o \left(1 + \alpha_{ij} \left(\frac{x_{ij}}{V_{ij}}\right)^{\beta_{ij}}\right) \tag{11}$$

$$v_{ij}(x_{ij}) = \frac{d_{ij}}{t_{ij}(x_{ij})} \tag{12}$$

To realize the complete potential of eco-routing freight, this work analyzes the network-wide impacts of eco-routing by developing a multi-class Traffic Assignment (TA) tool through an origin-based formulation, with the objective,

$$\min_{x_{ij}^{kr};\,(i,j) \in A} \quad z_k(\boldsymbol{x}) = \sum_{(i,j) \in A} \int_0^{x_{ij}^{kr} + x_{ij}^{kr-}} c_{ij}^k(u)\,du \quad \forall\ k \in K \tag{13}$$

Subject to,

$$x_{ij} = \sum_{r \in R} \sum_{k \in K} x_{ij}^{kr} \tag{14}$$

$$x_{ij}^{kr-} = x_{ij} - x_{ij}^{kr} \tag{15}$$

$$\sum_{n \in T(i)} x_{ni}^{kr} = \sum_{n \in H(i)} x_{in}^{kr} + q_i^{kr} \tag{16}$$

$$q_i^{kr} = \begin{cases} \sum_{s \in S_r} q_{rs}^k & \text{if } i \in R \\ -q_{rs}^k & \text{if } i \in S_r \\ 0 & \text{otherwise} \end{cases} \quad (17)$$

To solve this optimization problem, authors Lagrange transform the above formulation and consequently apply Karush-Kuhn-Tucker (KKT) conditions rendering,

$$\mathcal{L}_k(\boldsymbol{x}, \boldsymbol{u}) = z_k(\boldsymbol{x}) + \sum_{r \in R} \sum_{k \in K} \sum_{i \in N} u_i^{kr} \left( q_i^{kr} + \sum_{n \in H(i)} x_{in}^{kr} - \sum_{n \in T(i)} x_{ni}^{kr} \right) \quad (18)$$

Developing the KKT conditions,

$$x_{ij}^{kr} \frac{\partial \mathcal{L}_k}{\partial x_{ij}^{kr}} = 0; \quad \frac{\partial \mathcal{L}_k}{\partial x_{ij}^{kr}} \geq 0, x_{ij}^{kr} \geq 0 \quad (19)$$

$$\frac{\partial \mathcal{L}_k}{\partial x_{ij}^{kr}} = c_{ij}^k(x_{ij}) + u_i^{kr} - u_j^{kr} \quad (20)$$

$$x_{ij}^{kr} \pi_{ij}^{kr} = 0; \quad \pi_{ij}^{kr} \geq 0, x_{ij}^{kr} \geq 0 \quad (21)$$

Where, $\pi_{ij}^{kr}$ is the reduced cost for a vehicle, belonging to class $k \in K$, origination from node $r \in R$, for traversing arc $(i, j) \in A$, defined as $u_i^{kr} + c_{ij}^k(x_{ij}) - u_j^{kr}$. Here, $u_i^{kr}$ is the minimum travel cost for vehicle class $k \in K$ from origin $r \in R$ to node $i \in N$. The above-developed KKT conditions are akin to the classical Wardrop's equilibrium condition, wherein the cost of all traversed paths between an origin and a destination must be equal, and less than the cost of all untraversed paths between this origin and destination. Here, an analogous interpretation of the KKT condition suggests that all traversed arcs at equilibrium must have zero reduced cost (corresponding to the particular origin and vehicle class). Such an origin-based traffic assignment model was first formulated by Bar-Gera (2002), who later developed the Traffic Assignment by Paired Alternative Segments (TAPAS) algorithm (Bar-Gera, 2010) to get the assignment solution. Xie and Xie (2016) made further advancements, developing the improved TAPAS (iTAPAS).

This study expands the origin-based framework for multi-class traffic assignment, thus developing a multi-class TAPAS (mTAPAS). The fundamental idea behind the mTAPAS algorithm is to identify potential arcs, i.e., arcs that have a non-zero/substantial origin-based flow ($x_{ij}^{kr} > \epsilon$) and non-zero/substantial origin-based reduced cost ($\pi_{ij}^{kr} > \theta$), and to consequently adjust flow on these arcs. This flow shift occurs between Paired Alternative Segments (PAS), which are the sequence of arcs sharing a tail and a head node. Starting from the head node of the potential arc, the first segment traces back the least-cost path between origin and the head-node of the potential arc. The second segment on the other hand backtracks from the tail node of the potential arc, choosing predecessor nodes with maximum cost, until it converges with the least-cost path between origin and the head node of the potential arc. This renders a pair of sequence of arcs sharing a tail node at the point of intersection and a head node at the head of the potential arc. Once identified, flow is adjusted on the PAS based on Newton method (Dial, 2006). This process of identifying potential arcs and adjusting flow on the associated PAS

continues until the relative gap $(rg)$ falls below a pre-defined tolerance level, $tol$. Below is a brief description of the mTAPAS algorithm with the accompanying Maximum Cost Search (MCS) algorithm to establish PAS, and Newton Flow Shift (NFS) algorithm to perform flow shifts on the identified PAS. The implementation in this work employs $\epsilon = 10^{-12}$, $\theta = 10^{-16}$ and $tol = 10^{-6}$.

$$rg = 1 - \frac{\sum_{r\in R}\sum_{s\in S_r}\sum_{k\in K} q_{rs}^{k}.u_{rs}^{k}}{\sum_{r\in R}\sum_{k\in K}\sum_{(i,j)\in A} x_{ij}^{kr}.c_{ij}^{k}\left(\sum_{r\in R}\sum_{k\in K} x_{ij}^{kr}\right)} \quad (22)$$

This study employs Julia v1.4.2 (Bezanson et al., 2017) on an Intel Core i5-10210U CPU @ 1.60GHz PC to develop and run the traffic assignment algorithm. For a comprehensive description of the algorithm and corresponding Julia code, refer to the GitHub release (Pahwa, 2021).

**multi-class Traffic Assignment by Paired Alternative Segments (mTAPAS) –** $mTAPAS(\epsilon, \theta, tol)$

Step 1. Initialize origin-based arc flows $x_{ij}^{kr}$ and origin-based reduced arc cost $\pi_{ij}^{kr}$ at zero. Initialize an empty set $\rho$ to store Paired Alternative Segments (PAS).

Step 2. Perform All-or-Nothing (AON) assignment – From each origin $r$, find the least cost path to every destination $s$, for every vehicle class $k$, and assign demand $q_{rs}^{k}$ to this path. Update $x_{ij}^{kr}$ and $\pi_{ij}^{kr}$ for arcs on this path.

Step 3. Iterate until the algorithm converges

Step 3.1. Identify potential arcs, i.e., arcs with $x_{ij}^{kr} > \epsilon$ and $\pi_{ij}^{kr} > \theta$.

Step 3.2. For every potential arc, develop and store PAS in set $\rho$ using Maximum Cost Search (MCS) method.

Step 3.3. Perform flow shift on the identified PAS based on the Newton Method.

Step 3.4. Randomly sample a subset of PAS from set $\rho$ and perform flow shift to fasten algorithm convergence.

Step 4. Remove PAS which no longer results in significant improvement in the solution.

Step 5. If relative gap - $rg$, is smaller than the tolerance level - $tol$, go to Step 6, else repeat Step 3.

Step 6. Return origin-based arc flows $x_{ij}^{kr}$.

**Maximum Cost Search Algorithm (MCS) –** $mcs(a, k, r)$; $(i, j) \rightarrow a$

Step 1. Initialization

Step 1.1. Set status label $l_u$ to 1 for node $i$, -1 for all nodes on least cost path for vehicle class $k$ between origin node $r$ and node $j$, and 0 for all other nodes.

Step 1.2. Set predecessor label $L_u$ of node $j$ to node $i$, and to null for all other nodes.

Step 1.3. Set the tail and head node on arc $a$, $(t, h) \rightarrow a$.

Step 2. Iterate.

Step 2.1. Set the current node to the tail node, $v \rightarrow t$.

Step 2.2. Find the maximum cost arc headed on to the current node and set the tail and head node on this arc.

$$t, h \rightarrow \underset{n \in T(v)}{\operatorname{argmax}}\, c_{nv}^{k}, v$$

Step 2.3. Set the predecessor label of the current node to this tail node, $L_v \rightarrow t$

Step 2.4. If the tail node happens to be on the least cost path for vehicle class $k$ between origin node $r$ and node $j$, i.e., if $l_t = -1$ then the algorithm can establish a PAS.

Step 2.4.1. Establish the first segment of PAS - $e_1$, as the segment between the tail node $t$ and node $j$ on the least cost path for vehicle class $k$ between origin node $r$ and node $j$.

Step 2.4.2. Establish the second segment of the PAS - $e_2$, using predecessor labels, backtracking from node $j$ to the tail node $t$. Go to step 3.

Step 2.5. If the tail node is a previously identified predecessor, i.e., if $l_t = 1$, then the algorithm has found a cycle. Perform shift flow on this cycle based on Newton Method and restart the process from Step 1.

Step 2.6. Else update the status of the tail node to 1 and continue to step 2.1

Step 3. Return PAS $(e_1, e_2)$

**Newton Flow Shift (NFS) on PAS** $(e_1, e_2) - shift((e_1, e_2), k, r)$

Step 1. Set $c_1$ and $c_2$ as the sum of arc costs for vehicle class $k$ on $e_1$ and $e_2$ respectively.

Step 2. Set $c_1^{'}$ and $c_2^{'}$ as the sum of derivative* of arc cost for vehicle class $k$ on $e_1$ and $e_2$ respectively.

Step 3. Set $f_1$ and $f_2$ as the minimum arc flow for vehicle class $k$ from origin $r$ on $e_1$ and $e_2$ respectively.

Step 4. Compute $\Delta$ as $(c_2 - c_1)/(c_1^{'} + c_2^{'})$.

Step 5. Compute $\delta$ – if $\Delta \geq 0$ $\delta \rightarrow \min(f_2, \Delta)$ else $\delta \rightarrow \max(-f_1, \Delta)$.

Step 6. Add flow $\delta$ for arcs on $e_1$ and reduce flow $\delta$ for arcs on $e_2$, for vehicle class $k$ originating from node $r$

Step 7. Update reduced cost for arcs on $e_1$ and $e_2$, for vehicle class $k$ originating from node $r$.

* Derivative with respect to total arc flow

# IV. Case Study

This work develops an analysis for southern California, encompassing Imperial, Los Angeles, Orange, Riverside, San Bernardino, and Ventura counties, together forming the region administered by the Metropolitan Planning Organization (MPO) of Southern California Association of Governments (SCAG) (Figure 2). This region caters to some of the country's busiest freight terminals, such as the Port of Los Angeles (POLA), warehouses in San Bernardino, Los Angeles Airport (LAX) and more. The freight sector (retail trade/wholesale trade/transportation and warehousing) in this region employs about 20% of the work force, thus amounting to 16% of SCAG's GDP (US Census Bureau, n.d.). Table 2 offers county-wise insights into some of the region's relevant characteristics such as demography and economy.

**Figure 2. Southern California Council of Governments (SCAG) region – scope of this work**

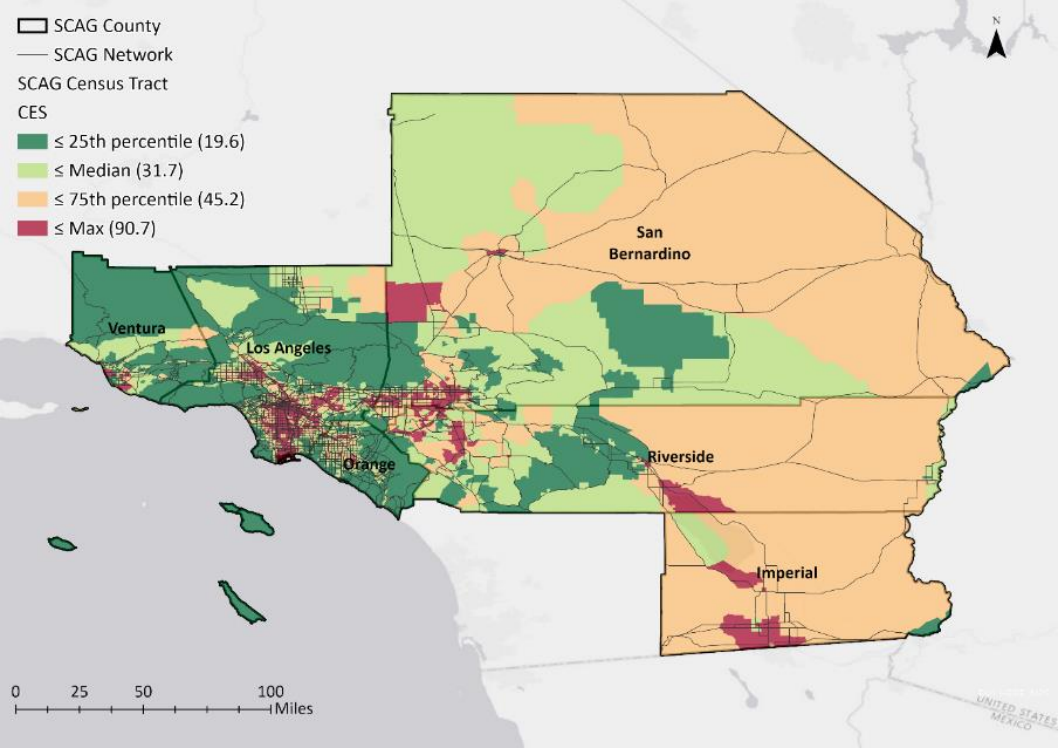


Network: Southern California Association of Governments (2016)
CalEnviroScreen scores: California Office of Environmental Health Hazard Assessment (2017)

While freight is essential for the economy, SCAG sustains a significant amount of freight traffic on its network, which brings along negative externalities such as congestion, emissions, and noise. Los Angeles county, for instance, with its relatively dense population and disadvantaged communities, faces adverse effects of transportation-related externalities. Emissions, specifically, Criteria Pollutants (CP) such as Carbon Monoxide (CO), Nitrogen Oxides ($NO_x$) and Particulate Matter (PM) have adverse negative health impacts on local communities, while Greenhouse Gases (GHGs) such as Methane ($CH_4$), Carbon Dioxide ($CO_2$), and Reactive Organic Gases (ROG) have implications on global climate change, and thus are studied in this work. To

establish vehicle emission rates for these pollutants, the authors employ the EMission FACtor (EMFAC) tool (California Air Resources Board (CARB), 2017) (Figure 3). See Appendix B for a comparison of emission rates for the average vehicle considered and those under the EMFAC Port of Los Angeles designation. For fuel consumption rates, the authors use the model developed by Scora et al. (2015) (Figure 4). Table 3 summarizes emission and fuel consumption rates for Heavy-Duty Trucks (HDT) and Light Duty Automobiles (LDA) (vehicle definitions from EMFAC), accounting for continuously differentiable, monotonically non-decreasing, and strictly positive properties of generalized cost function, as defined in the previous section

**Table 2. Relevant features of counties in the SCAG region**

| | Ventura | LA | SB | Orange | Riverside | Imperial |
|---|---|---|---|---|---|---|
| *Demographics* [a] | | | | | | |
| Population (million) | 0.85 | 10.1 | 2.14 | 3.16 | 2.38 | 0.18 |
| Land Area (sq. miles) | 1843 | 4058 | 20057 | 791 | 7206 | 4177 |
| Per capita income (thousand $) | $36.9 | $32.5 | $24.0 | $39.6 | $27.1 | $17.6 |
| Pop. density (per sq. mi.) | 460 | 2489 | 106 | 4002 | 331 | 43 |
| *Economy* [a] | | | | | | |
| GDP (billion $) | $53.4 | $710.9 | $85.1 | $230.1 | $79.8 | $8.0 |
| % GDP from freight sector | 13.7% | 15.0% | 22.7% | 16.0% | 18.1% | 13.5% |
| % Employed in freight sector | 16.9% | 19.6% | 25.9% | 17.6% | 22.2% | 22.8% |
| *Vulnerable* population [a] | | | | | | |
| % BPL | 9.6% | 16.0% | 17.3% | 11.5% | 14.7% | 24.2% |
| % Unemployed | 5.9% | 6.8% | 8.8% | 5.1% | 8.6% | 15.3% |
| % Young (age <= 9) | 12.4% | 12.2% | 14.7% | 12.0% | 13.7% | 15.9% |
| % Elderly (age >= 60) | 20.4% | 18.3% | 16.0% | 19.5% | 19.0% | 17.3% |
| *CalEnviroScreen (CES) Score* [b] | | | | | | |
| Avg. CES Score | 19.9 | 36.5 | 36.1 | 22.6 | 29.1 | 39.9 |
| Median CES Score | 18.0 | 36.4 | 36.5 | 21.1 | 27.8 | 39.6 |
| Max CES Score | 58.7 | 80.7 | 90.7 | 58.1 | 74.1 | 58.1 |

[a] US Census Bureau (n.d.)
[b] California Office of Environmental Health Hazard Assessment (2017)
CES Score is a pollution exposure index accounting for pollution burden and population characteristics.

For the first part of the analyses, this work evaluates the opportunities associated with eco-routing for a carrier hauling Heavy Duty Truck (HDT) fleet between different origin-destination pairs in the SCAG region with arc speeds following Weibull distribution (Figure 5) developed using HERE, a crowd-based platform (HERE Technologies, 2019). Given the stochastic nature of the network, this work assumes the carrier to make a priori choices of route with posterior realizations of arc speed, thus minimizing the expected cost of routing. For this carrier, the authors develop and compare the shortest path (SP), fastest path (FP), and least-cost path (LCP) with the eco-route being the one that minimizes expected emissions for different pollutants, i.e., the least-emissions path (LEP).

**Figure 3. Pollutant emission rates for Light-Duty Automobile (LDA) and Heavy-Duty Trucks (HDT)**

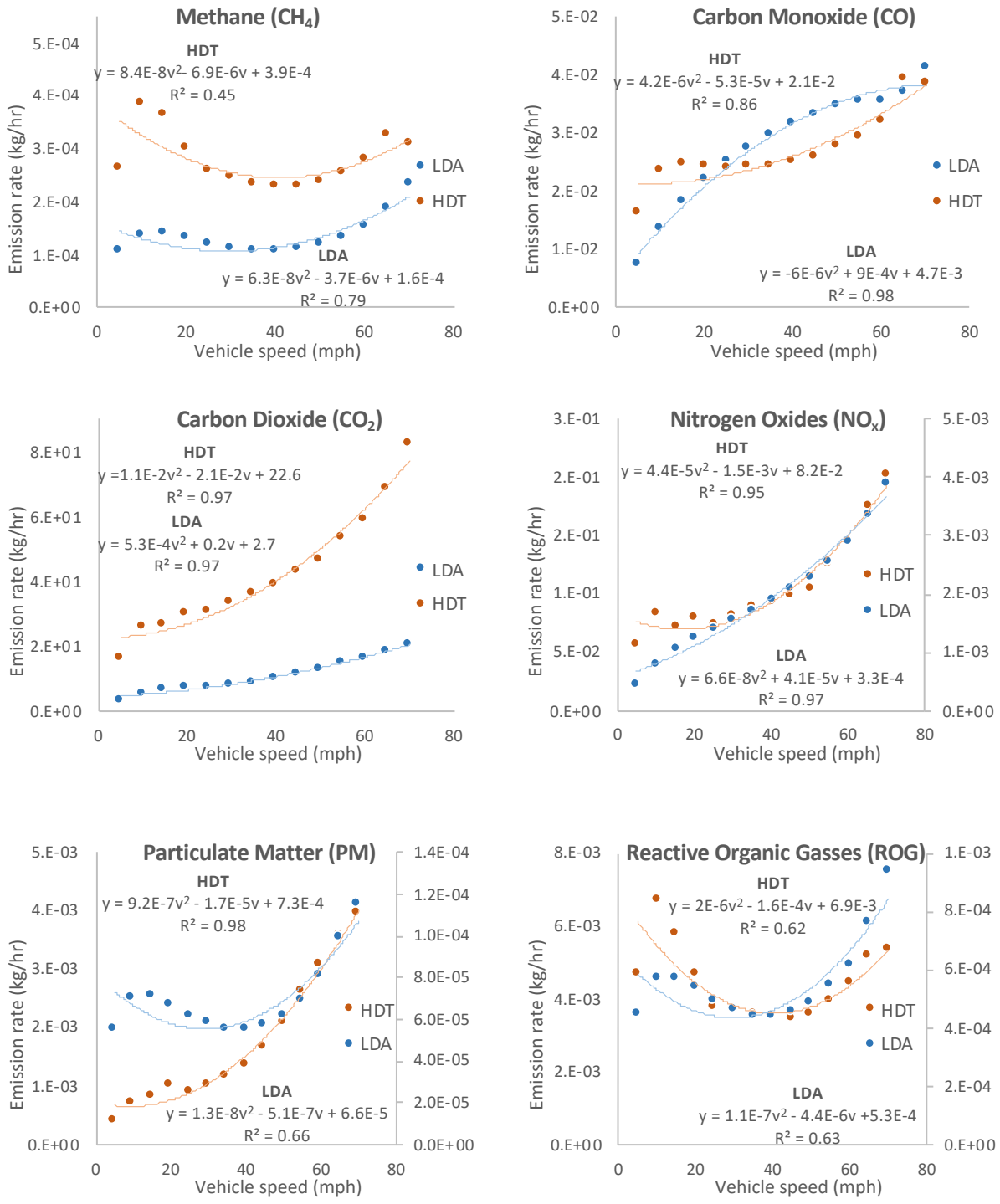


**Note:** Emission rates are for the SCAG region in 2020; Trendlines in the figure represents OLS model without accounting for continuously differentiable, monotonically non-decreasing, and strictly positive properties of the generalized cost function.

**Figure 4. Fuel consumption for Light-Duty Automobile (LDA) and Heavy-Duty Trucks (HDT)**

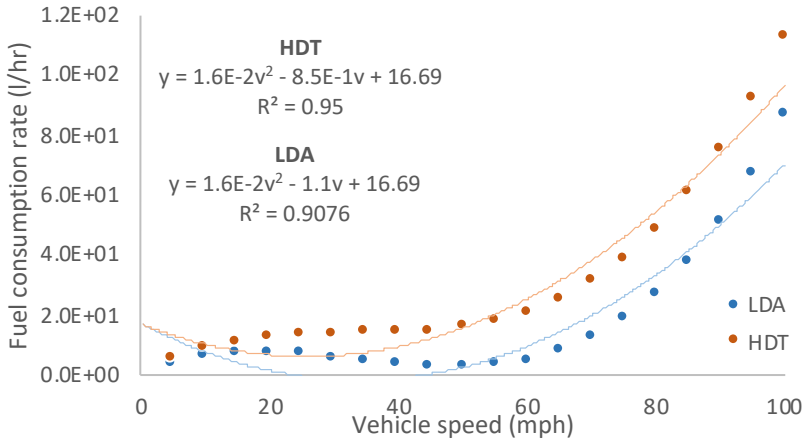


**Note:** Trendlines in the figure represents OLS model without accounting for continuously differentiable, monotonically non-decreasing, and strictly positive properties of the generalized cost function.

**Table 3. Emission and fuel consumption models**

| Parameter | Vehicle | $\eta^p_0$ | $\eta^p_1$ | $\eta^p_2$ | $R^2$ | Cost |
|---|---|---|---|---|---|---|
| *Fuel consumption* | | | | | | |
| FC | LDA | 8.48E+00 | -3.77E-01 | 8.29E-03 | 0.805 | $0.994/litre [a] |
| | HDT | 8.48E+00 | -1.13E-01 | 8.29E-03 | 0.884 | $1.051/litre [a] |
| *Criteria Pollutants (CPs)* | | | | | | |
| CO | LDA | 1.13E-02 | 4.39E-04 | 9.00E-08 | 0.919 | $0.199/kg [b] |
| | HDT | 2.14E-02 | -5.26E-05 | 4.16E-06 | 0.855 | |
| $NO_x$ | LDA | 3.30E-04 | 4.04E-05 | 6.55E-08 | 0.970 | $79.28/kg [b] |
| | HDT | 5.39E-02 | 8.98E-04 | 1.07E-05 | 0.864 | |
| PM | LDA | 6.62E-05 | -5.13E-07 | 1.31E-08 | 0.660 | $649.2/kg [b] |
| | HDT | 4.54E-04 | 3.37E-05 | 9.00E-08 | 0.855 | |
| *Green-House Gases (GHGs)* | | | | | | |
| $CH_4$ | LDA | 1.30E-04 | -1.04E-06 | 2.58E-08 | 0.632 | $1.781/kg [c] |
| | HDT | 3.78E-04 | -6.22E-06 | 7.50E-08 | 0.446 | |
| $CO_2$ | LDA | 2.66E+00 | 1.96E-01 | 5.28E-04 | 0.968 | $0.068/kg [c] |
| | HDT | 1.55E+01 | 5.78E-01 | 3.07E-03 | 0.940 | |
| ROG | LDA | 5.29E-04 | -4.35E-06 | 1.05E-07 | 0.628 | $4.925/kg [b] |
| | HDT | 6.21E-03 | -1.06E-04 | 1.23E-06 | 0.538 | |

Results from constrained OLS accounting for continuously differentiable, monotonically non-decreasing, and strictly positive properties of the generalized cost function.

[a] AAA Gas Prices (n.d.)

[b] Caltrans (2017)

[c] Environmental Protection Agency (EPA) (2019a)

**Figure 5. Class-wise histogram and best fit Weibull distribution of observed vehicle speeds**

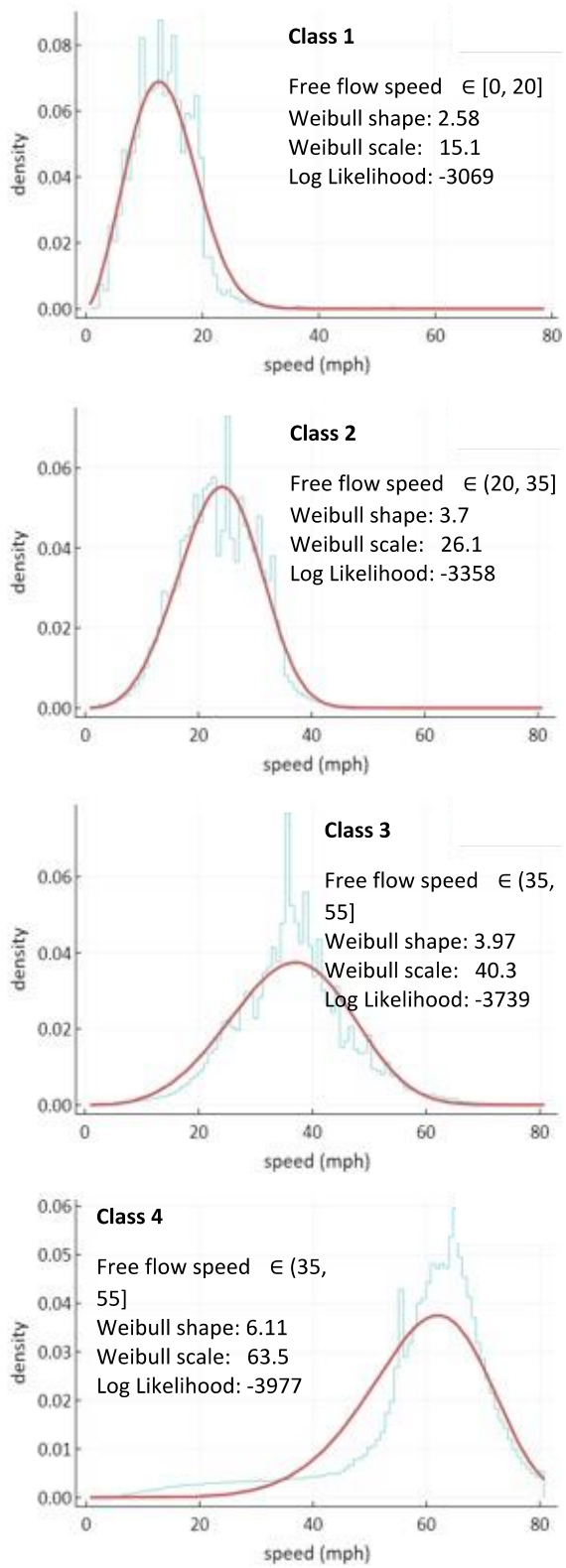

In the second part of the analyses, the authors develop network-wide effects using traffic assignment for the SCAG network with two vehicle classes: Light Duty Automobile (LDA), i.e., passenger cars, and Heavy-Duty Trucks (HDT). While the passenger cars route on the fastest path, the trucks can route on the shortest path (SP assignment), fastest path (FP assignment), least-cost path (LCP assignment), or on the least-emissions path (LEP assignment). In addition to estimating the network-wide effects of eco-routing, this work explores eco-routing's impacts on disadvantaged communities identified using CalEnviroScreen score (Figure 6). Moreover, the authors develop and compare SP, FP and LCP assignments with and without geofencing for these identified disadvantaged communities.

**Figure 6. Identified disadvantaged communities**

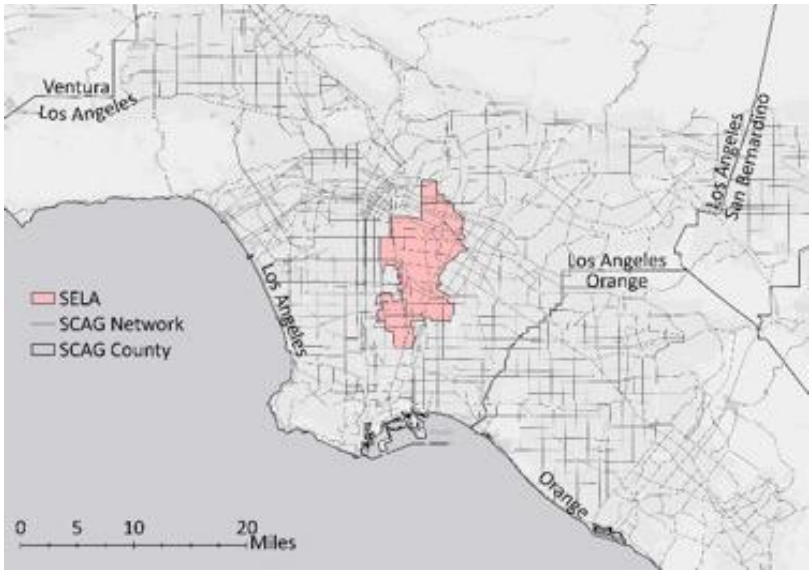


a) South East LA

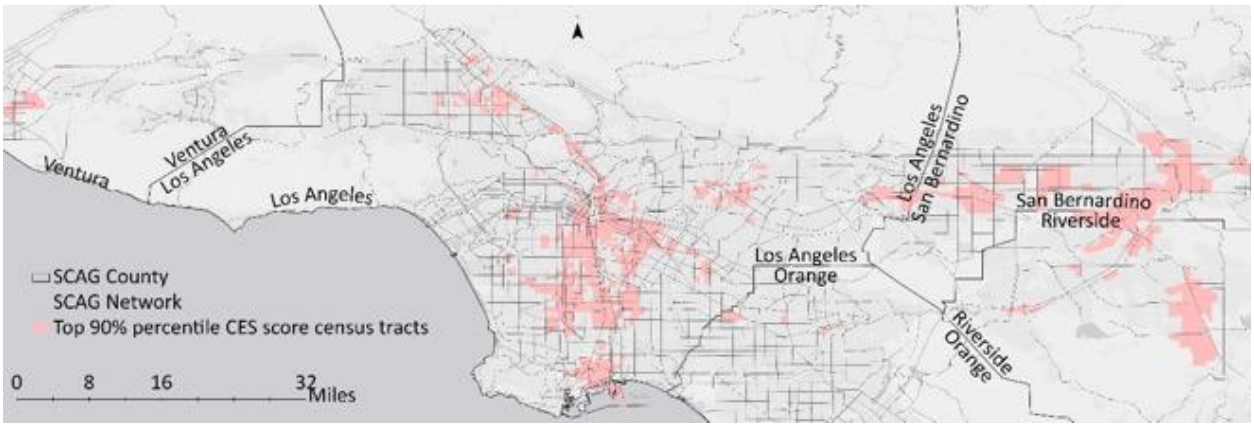


b) High CES score census tracts

# V. Empirical analysis of eco-routing

## Private impacts

The first part of the analyses deals with the cost-benefits of eco-routing for a carrier hauling to different destinations in the SCAG region from the Port of LA (POLA). In particular, the authors compare the costs and benefits of eco-routing (least emissions path - LEP) with conventional routing options such as the shortest path (SP), fastest path (FP) and the least-cost path (LCP). The "cost" in the least-cost path, referred to as "travel cost" from here on, accounts for travel distance, travel time and fuel consumed. The benefits of eco-routing pertain to reductions in emissions realized from eco-routing, while the cost of eco-routing is contextual to the conventional routing option in comparison. The cost of eco-routing pertains to increase in travel distance when compared with shortest path, travel time when compared with fastest path, and travel cost when compared with least-cost path. Authors here assume a stochastic network; wherein arc speeds follow a Weibull distribution (Figure 5). Additionally, the analysis assumes a carrier making a priori plans for routing its fleet with posterior realizations of arc costs, thus minimizing its expected cost of routing.

To begin with, the analysis here presents a comparison of carbon-dioxide eco-routing (LEP - $CO_2$) with the three conventional routing options for freight trips between POLA and San Bernardino (SB) (Table 4, Figure 7, Figure 8 and Figure 9). Due to the stochastic nature of arc speeds, the travel time, amount of fuel consumed, and emissions also exhibit a probabilistic nature. In each of the three figures, the expected benefits can be seen to be counterbalanced by the expected cost of eco-routing, though the magnitudes of the respective costs and benefits differ across the three. This is evident by the three tables comparing eco-routing with conventional routing options for all trips from POLA to different destinations in the SCAG region (see column 2 and 3 of Table 5, Table 6 and Table 7). The increase in carrier's costs due to eco-routing suggest a lack of incentive for the carrier to carry out eco-friendly routing. Though a reduction in other parameters (see Table 5), could motivate that carrier to eco-route.

In general, the costs and benefits of eco-routing are significant in the context of shortest path routing. In comparison with the other two conventional options, the costs and benefits of eco-routing are relatively modest. On a further cost-benefit analysis, taking $\log_{10}$(cost/benefit), almost none of the eco-routes render a net monetary gain for the carrier and society combined. Benefits to the society from a reduction in emissions due to carrier eco-routing are compensated for by an increase in cost to the carrier from eco-routing. Only if the carrier would otherwise route its fleet for shortest distance, does $NO_x$ eco-routing (eco-route minimizing $NO_x$ emissions) render a higher monetary benefit for society than the monetary cost to the carrier, as reflected by the -0.19 value in Table 5. In fact, the cost-benefit values from the tables reflect an emission cost factor (in the order of 10) that can balance, or break even, the costs and benefits of eco-routing. Currently $NO_x$ is valued at \$79.28/kg, however, for $NO_x$ eco-route to break even with least cost path, monetary benefits to the society from $NO_x$ reduction must be 10 times higher, at \$792.8/kg (see Table 7). Thus, considering the cost-benefit values, the order of best-to-worst eco-route is $NO_x$, $CO_2$, PM, ROG, CO, $CH_4$, across all the three comparisons.

**Table 4. Description of POLA to SB routes**

| Route | # Arcs | Arc capacity (PCU/hr) | Arc length (mi) | Arc FFT (hr) | % Car traffic | % Truck traffic |
|---|---|---|---|---|---|---|
| SP | 85 | 1324 | 0.799 | 0.029 | 72.5% | 27.6% |
| FP | 143 | 1254 | 0.586 | 0.014 | 80.8% | 19.2% |
| LCP | 121 | 1236 | 0.625 | 0.017 | 80.0% | 20.0% |
| LEP-$CO_2$ | 74 | 1114 | 1.194 | 0.047 | 75.4% | 24.6% |

All arc values are average values on the route. PCU – Passenger Car Unit, FFT – Free Flow Travel Time

**Figure 7. Carbon Dioxide eco-routing (LEP - $CO_2$) vs. shortest path routing (SP) – POLA to SB**

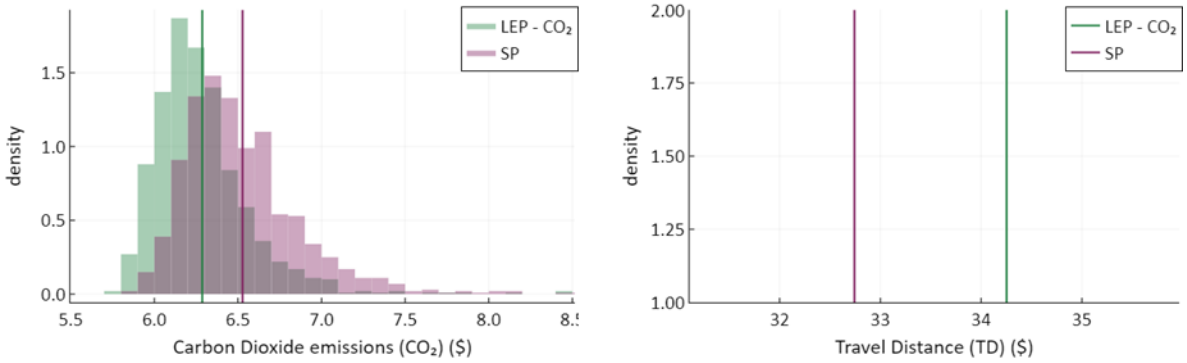


**Figure 8. Carbon Dioxide eco-routing (LEP - $CO_2$) vs. fastest path routing (FP) – POLA to SB**

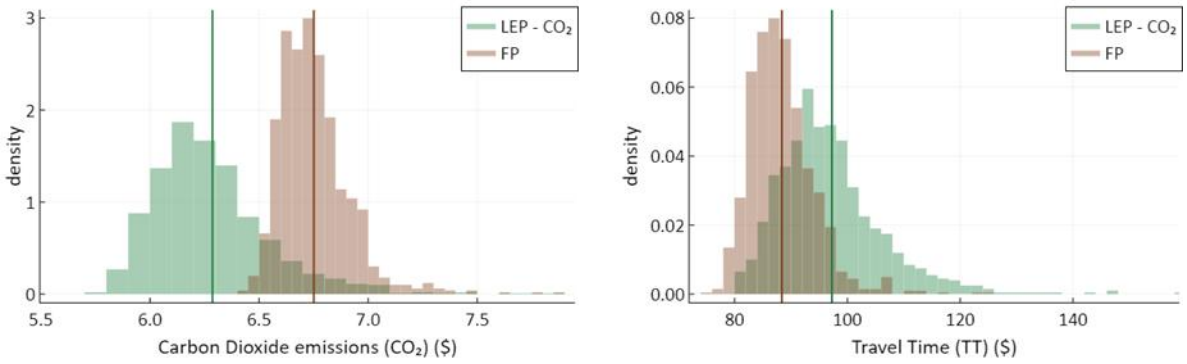


**Figure 9. Carbon Dioxide eco-routing (LEP - $CO_2$) vs. least-cost routing (LCP) – POLA to SB**

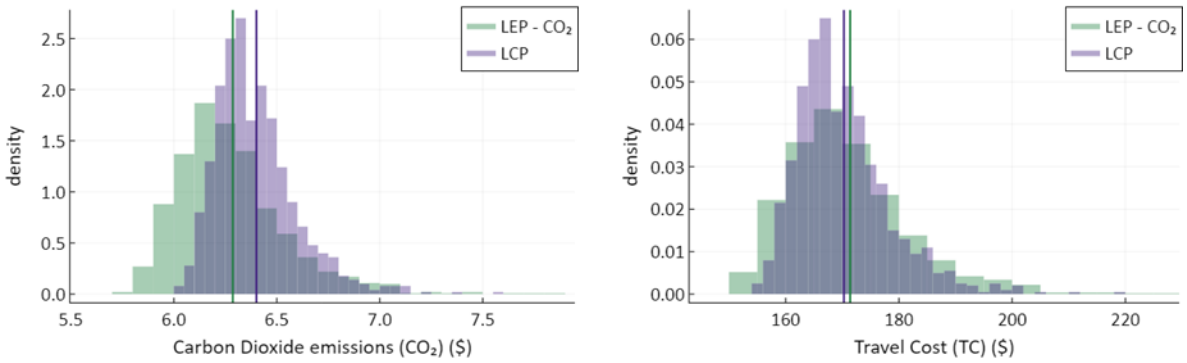

**Table 5. Least Emissions Path (LEP) vs. Shortest Path (SP)**

| Pollutant | % ΔTD | % ΔE | % ΔTT | % ΔFC | Cost-Benefit |
|---|---|---|---|---|---|
| $CH_4$ | 13.3% | -21.1% | -17.5% | 1.4% | 3.86 |
| CO | 6.3% | -13.6% | -16.7% | -3.9% | 2.87 |
| $CO_2$ | 3.9% | -6.3% | -15.8% | -4.9% | 0.44 |
| $NO_x$ | 4.4% | -9.0% | -16.2% | -4.7% | -0.19 |
| PM | 2.8% | -3.8% | -14.6% | -5.0% | 1.01 |
| ROG | 14.1% | -21.6% | -17.4% | 2.0% | 2.23 |

Cost of eco-routing – $\theta_{TD} . \Delta TD$, Benefit of eco-routing – $\theta_E . \Delta E$, Cost-Benefit – $\log_{10}$(Cost/Benefit)

**Table 6. Least Emissions Path (LEP) vs. Fastest Path (FP)**

| Pollutant | % ΔTT | % ΔE | % ΔTD | % ΔFC | Cost-Benefit |
|---|---|---|---|---|---|
| $CH_4$ | 0.06% | -0.03% | 0.58% | 0.42% | 5.13 |
| CO | 1.1% | -0.63% | -4.9% | -4.3% | 4.10 |
| $CO_2$ | 2.2% | -3.5% | -6.9% | -5.2% | 0.93 |
| $NO_x$ | 1.8% | -2.4% | -6.5% | -5.0% | 0.57 |
| PM | 3.9% | -4.8% | -7.8% | -5.3% | 1.39 |
| ROG | 0.13% | -0.08% | 1.4% | 1.0% | 3.37 |

Cost of eco-routing – $\theta_{TT} . \Delta TT$, Benefit of eco-routing – $\theta_E . \Delta E$, Cost-Benefit – $\log_{10}$(Cost/Benefit)

**Table 7. Least Emissions Path (LEP) vs. Least Cost Path (LCP)**

| Pollutant | % ΔTC | % ΔE | % ΔTD | % ΔTT | % ΔFC | Cost-Benefit |
|---|---|---|---|---|---|---|
| $CH_4$ | 2.1% | -2.2% | 7.8% | -1.2% | 6.0% | 4.98 |
| CO | 0.18% | -0.04% | 1.2% | -0.26% | 0.54% | 4.14 |
| $CO_2$ | 0.16% | -0.25% | -1.0% | 0.89% | -0.49% | 1.15 |
| $NO_x$ | 0.04% | -0.04% | -0.54% | 0.40% | -0.28% | 1.00 |
| PM | 0.85% | -0.70% | -2.0% | 2.5% | -0.59% | 1.82 |
| ROG | 2.4% | -2.4% | 8.7% | -1.2% | 6.6% | 3.35 |

Travel cost (TC) – $\theta_{TD} . TD + \theta_{TT} . TT + \theta_{FC} . FC$, Cost of Eco-routing – $\theta_{TD} . \Delta TD + \theta_{TT} . \Delta TT + \theta_{FC} . \Delta FC$, Benefit of eco-routing – $\theta_E . \Delta E$, Cost-Benefit – $\log_{10}$(C/B)

In addition to the expected costs and benefits from eco-routing, this work also reflects on the reliability aspect of eco-routing, owing to the stochastic nature of the network. In particular, the analysis looks at emission (E), travel distance (TD), travel time (TT), fuel consumption (FC) and travel cost (TC) reliability. To measure reliability, the authors employ two metrics– coefficient of variation and inter-decile range. While the former reflects on the deviation around the mean, the latter represents the range. A smaller value in either metric reflects better reliability. Based on the discussion above, emission reliability is worst on the shortest path, best on fastest path, with the eco-route and least-cost paths as close 2nd or 3rd best (Table 8 and Table 9). While the order of best-to-worst eco-route for travel time, fuel consumption and travel cost reliability is $CH_4$, ROG, CO, $NO_x$, $CO_2$, PM (Table 10 and Table 11). Travel

distance reliability is mentioned for the sake of thoroughness. All of the results discussed above are weighted by demand between the origin-destination pairs.

**Table 8. Emission reliability – coefficient of variation**

| Pollutant | SP | FP | LCP | LEP |
|---|---|---|---|---|
| $CH_4$ | 0.21 | 0.13 | 0.15 | 0.13 |
| CO | 0.16 | 0.09 | 0.10 | 0.10 |
| $CO_2$ | 0.09 | 0.04 | 0.05 | 0.06 |
| $NO_x$ | 0.12 | 0.06 | 0.07 | 0.08 |
| PM | 0.07 | 0.03 | 0.04 | 0.05 |
| ROG | 0.21 | 0.14 | 0.15 | 0.13 |

**Table 9. Emission reliability – log of inter-decile range**

| Pollutant | SP | FP | LCP | LEP |
|---|---|---|---|---|
| $CH_4$ | -3.38 | -3.71 | -3.65 | -3.71 |
| CO | -2.58 | -2.91 | -2.84 | -2.85 |
| $CO_2$ | -0.19 | -0.52 | -0.45 | -0.41 |
| $NO_x$ | 0.42 | 0.09 | 0.16 | 0.19 |
| PM | -0.74 | -1.07 | -1.00 | -0.94 |
| ROG | -1.73 | -2.05 | -1.99 | -2.06 |

**Table 10. Eco-route reliability – coefficient of variation**

| Path | TD | TT | FC | TC |
|---|---|---|---|---|
| LEP - $CH_4$ | 7.30E-16 | 0.10 | 0.05 | 0.07 |
| LEP - CO | 7.22E-16 | 0.12 | 0.07 | 0.08 |
| LEP - $CO_2$ | 7.23E-16 | 0.13 | 0.08 | 0.09 |
| LEP - $NO_x$ | 7.29E-16 | 0.12 | 0.07 | 0.09 |
| LEP - PM | 7.28E-16 | 0.14 | 0.08 | 0.10 |
| LEP - ROG | 7.24E-16 | 0.10 | 0.05 | 0.07 |

**Table 11. Eco-route reliability – log of inter-decile range**

| Path | TD | TT | FC | TC |
|---|---|---|---|---|
| LEP - $CH_4$ | -14.52 | 1.04 | 0.37 | 1.10 |
| LEP - CO | -14.79 | 1.10 | 0.43 | 1.16 |
| LEP - $CO_2$ | -14.85 | 1.14 | 0.47 | 1.21 |
| LEP - $NO_x$ | -14.86 | 1.13 | 0.46 | 1.20 |
| LEP - PM | -14.81 | 1.16 | 0.50 | 1.23 |
| LEP - ROG | -14.55 | 1.04 | 0.37 | 1.10 |

## System impacts

### Truck eco-routing

Having established the impacts of eco-routing for the carrier, in the second part of the analyses the authors consider the network-wide impacts of eco-routing through traffic assignment. The analysis here assumes two class of vehicles: light-duty automobile (LDA), i.e., passenger cars, and heavy-duty trucks (HDT), i.e., delivery trucks. While the passenger cars in the network each minimize their travel time, the delivery trucks, as in the previous section, will minimize either their travel distance, travel time, travel cost, or emissions. For the sake of simplicity, the analysis here refers to each of the assignments as SP assignment, FP assignment, LCP assignment and LEP assignment, respectively, indicating the particular routing decision for the delivery truck, while passenger cars continually minimize travel time.

In a preliminary analysis, authors found insignificant network-wide reductions in emissions from eco-routing trucks. However, given that 95% of the traffic is passenger cars, such a modest result is unsurprising. Thus, to better evaluate the possibilities of eco-routing, the authors carry out a traffic assignment analysis at different congestion levels of passenger cars. Figure 10 presents the reduction in network-wide emissions from eco-routing delivery trucks (LEP assignment) in comparison with a SP, FP, and LCP assignment, respectively, for different passenger car congestion levels. The congestion level essentially reflects a multiplicative factor for passenger car demand between origin-destination pairs relative to the current level of demand. Much like in the previous subsection, the network-wide reductions in emissions from LEP assignment are significant in the context of the SP assignment; peaking in the absence of passenger cars in the network (Figure 10a), but relatively moderate when compared to the FP and LCP assignment; wherein the emission reductions peak for an optimal level of passenger car congestion in the network (Figure 10b,c). For most part, eco-routing trucks renders a reduction in network-wide emissions, with the exception of a few cases. For instance, eco-routing trucks to minimize $CO_2$ emissions in place of minimizing travel costs results in a net increase in network-wide carbon-dioxide emissions, at certain passenger car congestion levels. This increase in network-wide emissions is due to a significant increase in passenger car emissions despite a reduction in truck emissions. Authors observe a similar opposite effect for Vehicle Miles Traveled (VMT); a reduction in truck VMT is compensated for by an increase in passenger car VMT, and vice-versa, leading to a net increase/decrease in network-wide VMT depending on the passenger car congestion level in the network (see Appendix C).

Understanding such micro-level variations is essential to understanding the full system-wide potential of eco-routing. Figure 11 presents these spatial impacts of eco-routing on the network for certain pollutants. And while the SCAG region as a whole realizes a reduction in emissions owing to eco-routed trucks as discussed above, certain parts of the region may observe an increase in emissions. However, such spatial variations in the emissions did not disproportionately affect, either negatively or positively, disadvantaged communities in the SCAG region. Thus, certain disadvantaged communities observed an increase in emissions, while other disadvantaged communities in equal effect observed a reduction in emissions.

**Figure 10. Network-wide reduction in emissions from eco-routing trucks**

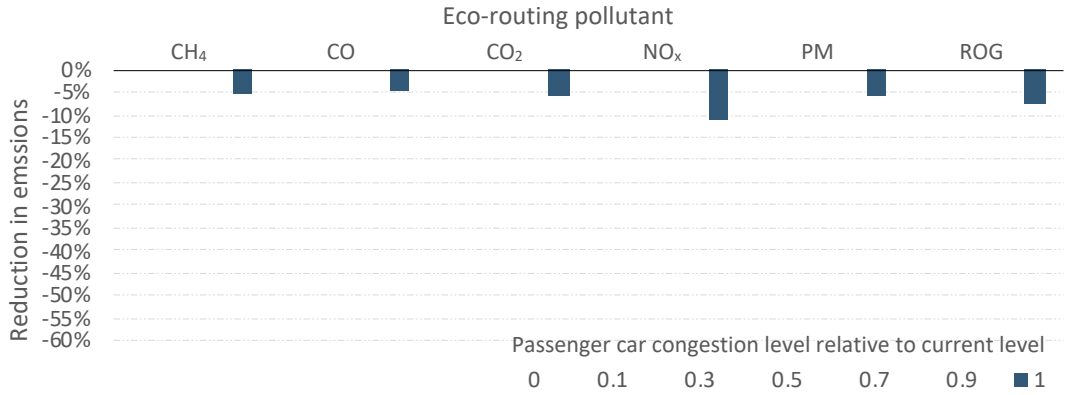


a) LEP assignment vs. SP assignment

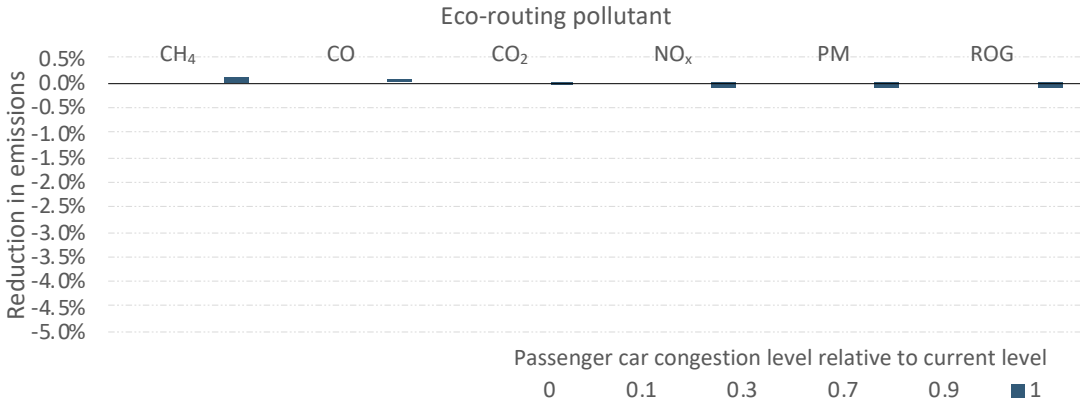


b) LEP assignment vs. FP assignment

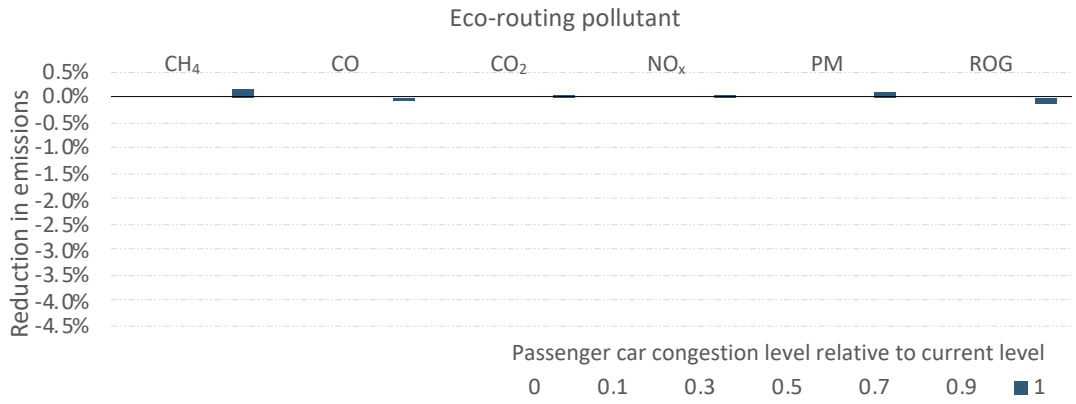


c) LEP assignment vs. LCP assignment

**Figure 11. Spatial effects of eco-routing**

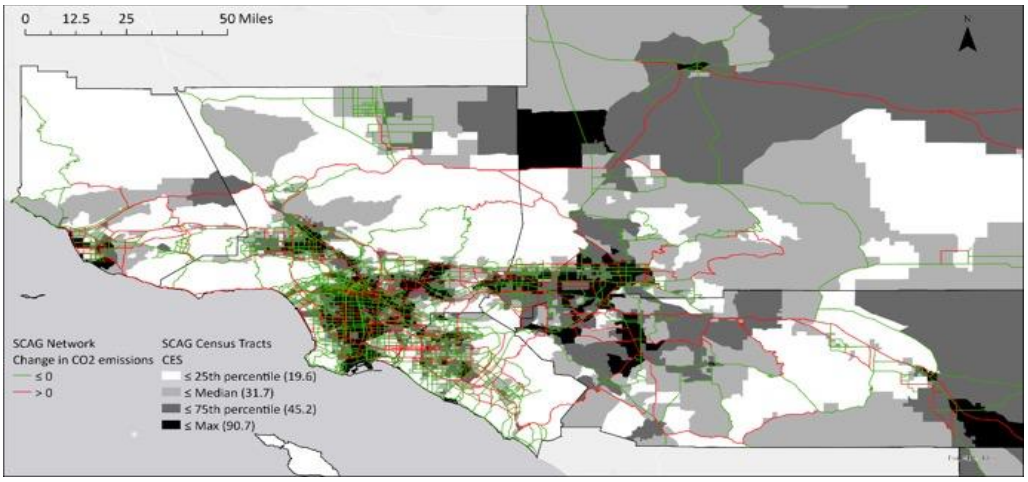


a) LEP-$CO_2$ assignment vs. SP assignment – Change in $CO_2$ emissions

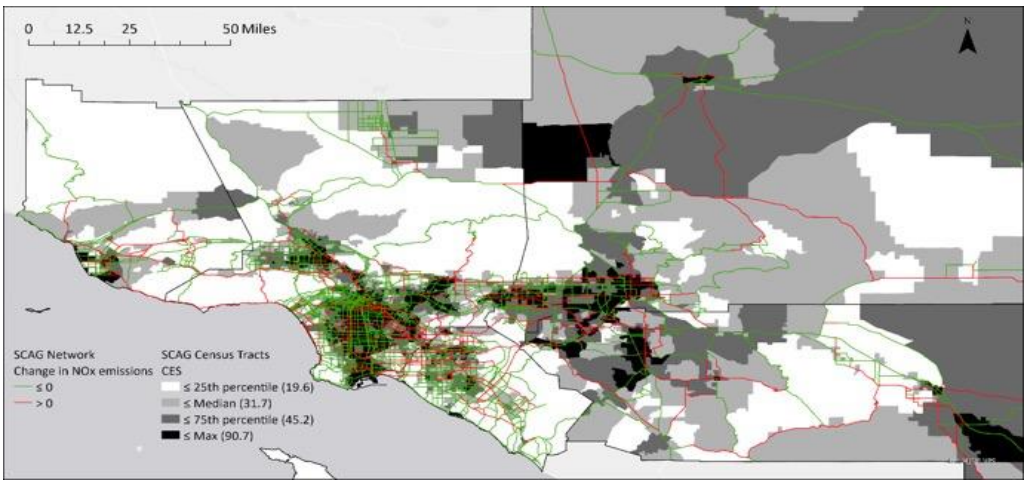


b) LEP-$NO_x$ assignment vs. FP assignment – Change in $NO_x$ emissions

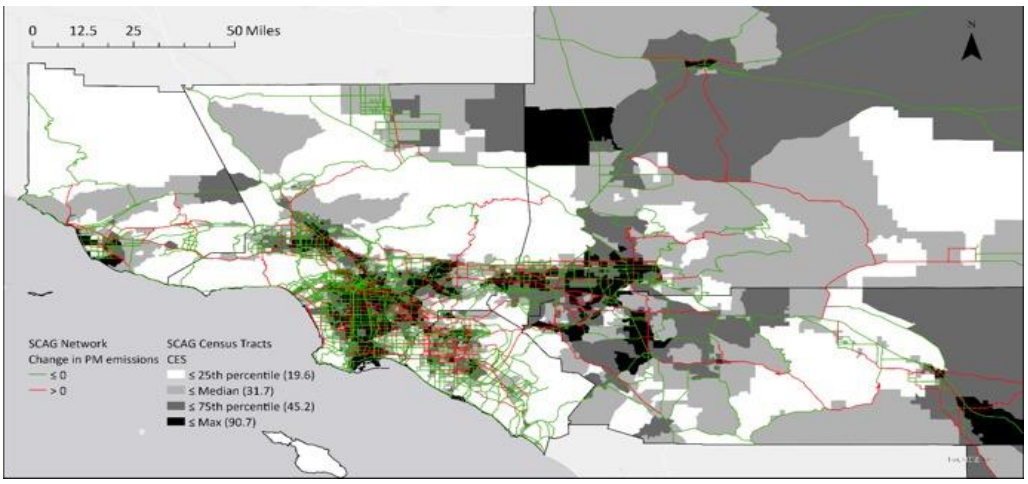


c) LEP-PM assignment vs. SP assignment – Change in PM emissions

## Geofencing South East Los Angeles (SELA)

In addition to the network-wide effects of eco-routing, this work assesses impacts for the South East LA (SELA) region, a disadvantaged region identified using CalEnviroScreen for the purpose of this work (Figure 6a). At current traffic demand levels, certain pollutant emissions within the SELA region may increase as a consequence of trucks eco-routing in the network. For instance, $NO_x$ and PM emissions in the SELA region increase by 5.1% and 17.8%, respectively, due to eco-routing in comparison to least-cost routing. Thus, in order to reduce the emission burden on disadvantaged communities like SELA, in this case, this work proposes geofence as an alternate eco-friendly routing mechanism. As explored in the previous subsection, the carrier currently has no direct incentive to eco-route and reduce emissions, however, imposing a fee for traveling within the disadvantaged region can bring about some of the desired reductions in emissions impacting the disadvantaged region. The fee considered in this work is a per-mile fee when trucks route for shortest path (SP assignment), a per-hour fee when trucks route for fastest path (FP assignment), and a combined per-mile, per-hour and per-gallon of diesel fee when trucks route for the least-cost path (LCP assignment). Thus, the carrier observes the operational cost and an additional fee, as described above, when traveling within the geofenced region.

Figure 12 shows the change in externalities, i.e., Vehicle Miles Traveled (VMT), Vehicle Hours Traveled (VHT), Vehicle Energy Consumed (VEC) and emissions, within the SELA region due to geofencing, for SP, FP and LCP assignment at different levels of geofence fee. As is evident from the figure, geofencing can bring about significant reductions in emissions in the SELA region, with the most notable reductions in $NO_x$ emissions followed by ROG, PM, $CO_2$, $CH_4$ and with the least reductions in CO emissions. Other externalities, such as VMT, VHT and VEC, may increase owing to increased passenger car traffic within the SELA region, though the magnitude of increase is quite moderate compared to the magnitude of emission reductions. On the network-wide scale, geofencing the SELA region makes only a marginal impact, with at most 1% increase in emissions in the worst case ($NO_x$ emissions, which increase by 0.83% network-wide for the SP assignment). Yet, it is important to note that a reduction in emissions in the SELA region brings along an increase in emissions in other parts of the region, as is the case with the outer census tracts adjoining the SELA region (Figure 13). For instance, under the LCP assignment, geofencing SELA with a large geofence fee, reduces $NO_x$ emissions within the SELA region by about 74%, but at the same time 14% of the links in the network experience a more than 100% increase in $NO_x$ emissions, while 4.4% of the links observe a ten-fold increase. Under the SP and FP assignments, the corresponding numbers are 7.6%, 2.6% and 18%, 3.5% respectively. Yet, these impacts, as discussed earlier, are not disproportional with respect to CES scores. Therefore, at any level of CES score, one can find a census tract (excluding the geofence) with as much reduction in emissions as increase in emissions in another census tract. Thus, geofencing can bring about a desired outcome in the form of a reduction in emissions for the disadvantaged region with a minimal but equitable increase in network-wide emissions.

**Figure 12. Local impacts of geofencing South-East LA (SELA) region**

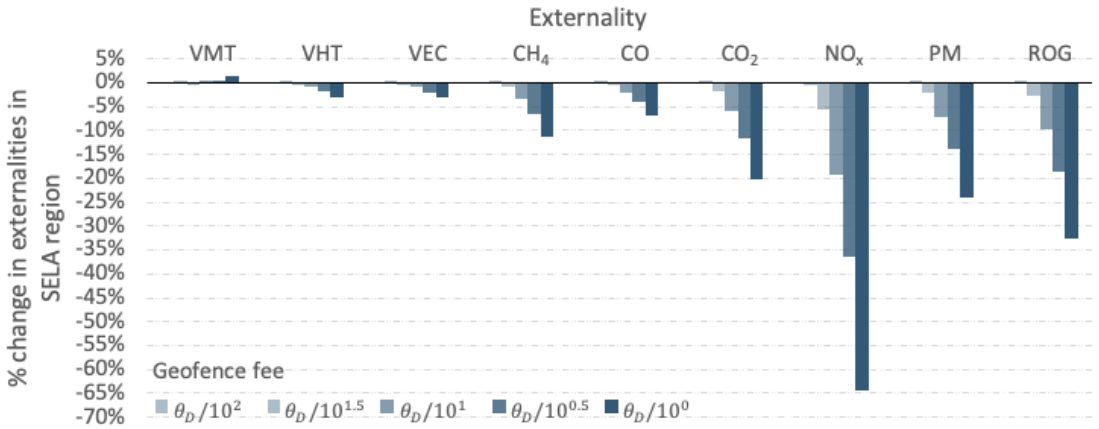


a) SP assignment- with vs. without SELA geofence

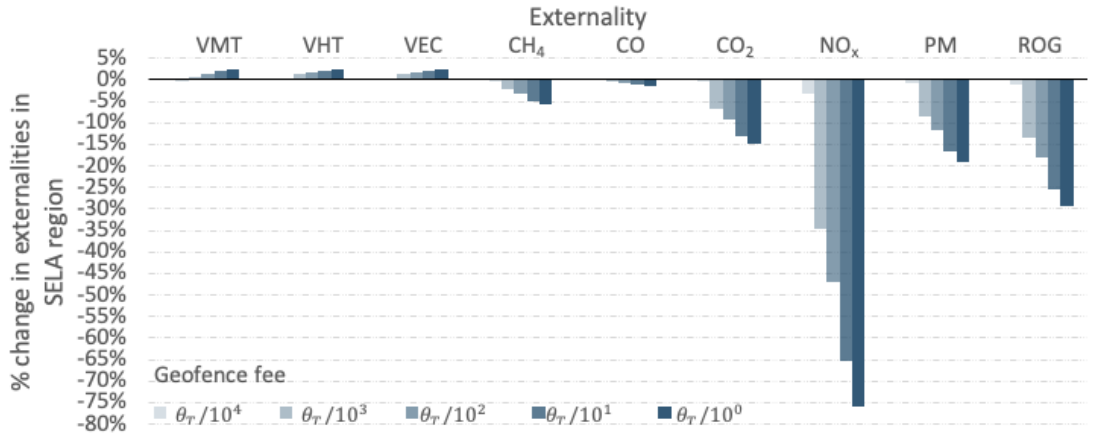


b) FP assignment- with vs. without SELA geofence

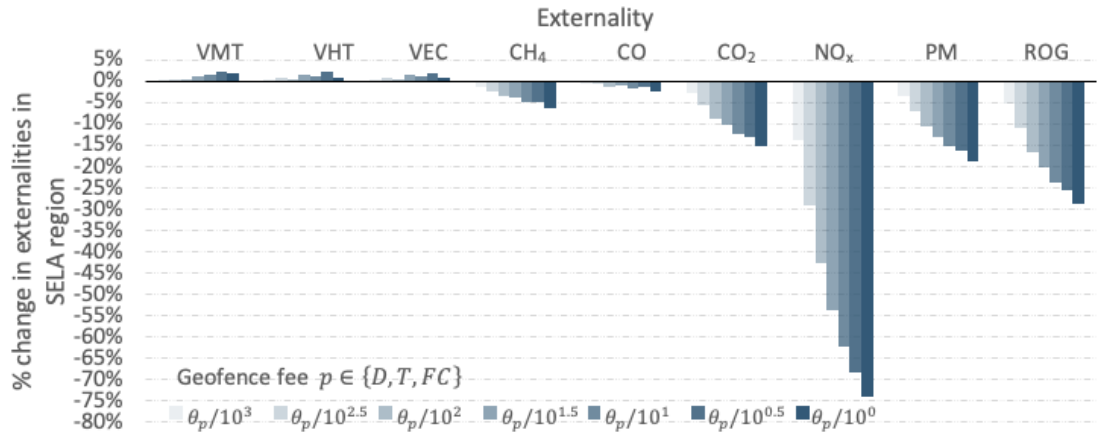


c) LCP assignment- with vs. without SELA geofence

**Figure 13. Spatial effects of geofencing SELA region**

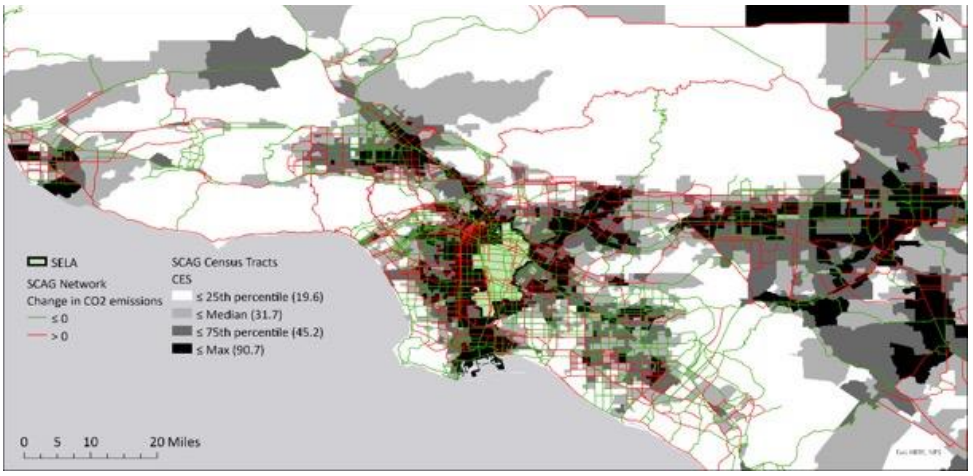


a) SP assignment- with vs. without SELA geofence – Change in $CO_2$ emissions

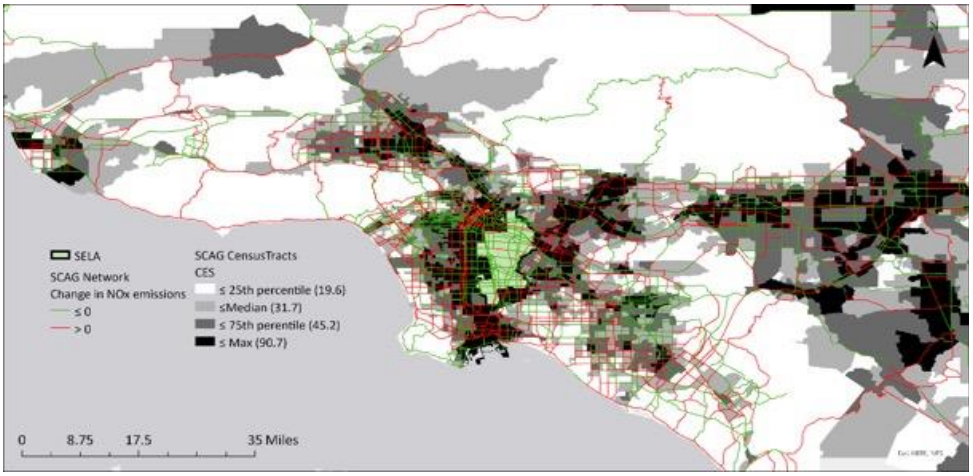


b) FP assignment- with vs. without SELA geofence – Change in $NO_x$ emissions

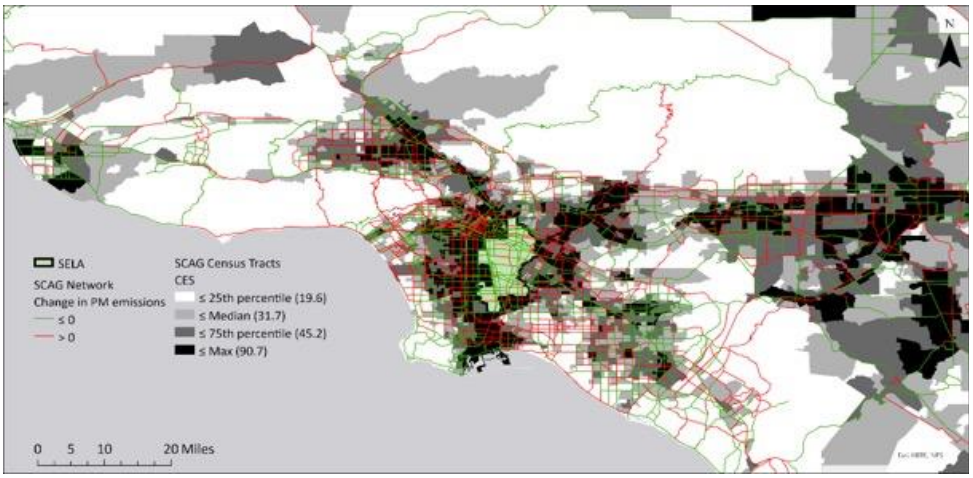


c) LCP assignment- with vs. without SELA geofence – Change in PM emissions

### Geofencing high CalEnviroScreen score census tracts

For the final part of the analyses, the authors carry out a geofencing exercise similar to the SELA exercise, restricting truck movement in the high CalEnviroScreen (CES) score census tracts, i.e., census tracts falling in the high 90%ile for the CES score (Figure 6b) by raising costs for the carrier to operate in this region. These census tracts, when put together, amount to a larger geofenced area than the SELA region, however, unlike the SELA region, the identified census tracts do not form a contiguous and continuous space. Thus, establishing and implementing a geofence "around" such a region may not be viable, nevertheless, the purpose of this analysis is to establish an extreme case of geofencing. The geofence fee levied on the carrier is as much as the operational cost to the carrier for operating within the geofence.

Figure 14 presents network-wide and local impacts of geofencing. The reduction in externalities within the geofence region falls in a similar range and follows a similar pattern as those associated with the SELA geofence. $NO_x$ emissions observe the most reduction, followed by ROG, PM, $CO_2$, $CH_4$, while CO emissions show the least reduction. However, due to the larger size and spread of this geofence region compared with the SELA geofence, the network is slightly more impacted. $NO_x$ emissions, in particular, may increase by 1%-5% network-wide due to restricted truck movements in the geofence. And since $NO_x$ is a criteria pollutant, the spatial spread of this increase could be critical. For instance, the 84% drop in $NO_x$ emissions in the geofence under FP assignment brings about a simultaneous rise in $NO_x$ emissions in 42% of the census tracts. However, the more disadvantaged census tracts (excluding the geofence) observed a small but statistically insignificant drop in emissions, as discussed in the previous subsections/analyses. Thus, as noted previously, geofencing can bring about the desired reduction in emissions for the geofenced region, with marginal but equitable increase in network-wide emissions (Figure 15).

**Figure 14. Network-wide and local impacts of geofencing high CES census tracts**

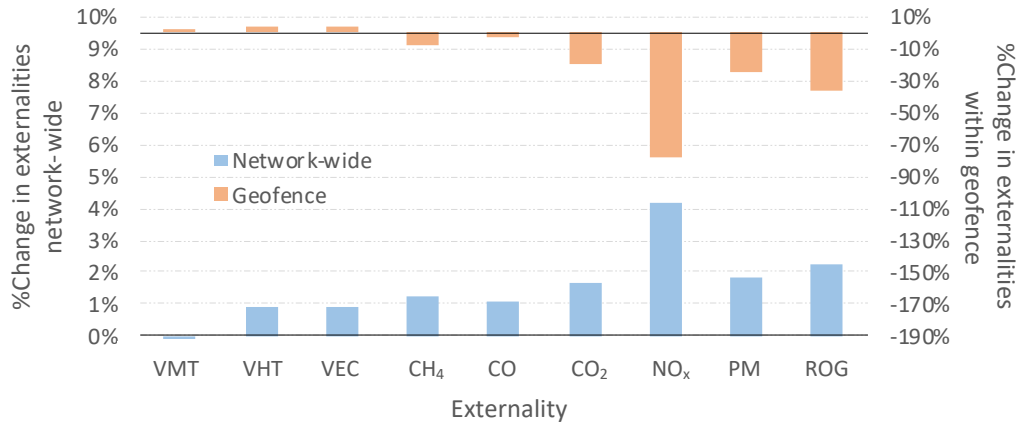


a) SP assignment- with vs. without geofence

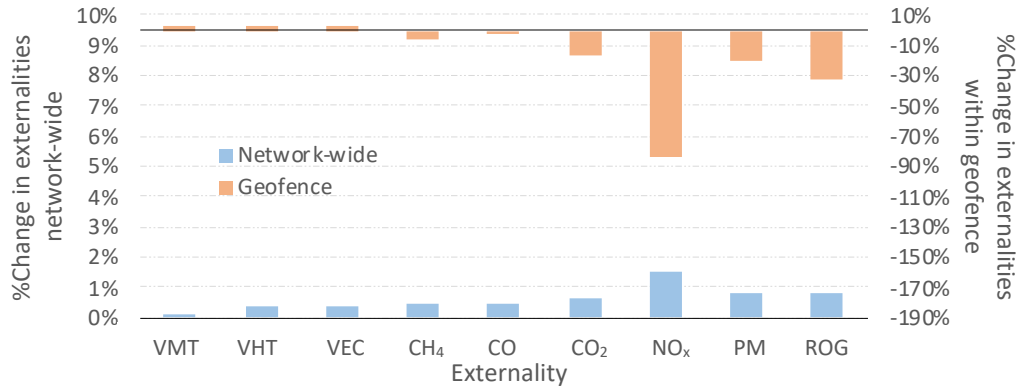


b) FP assignment- with vs. without geofence

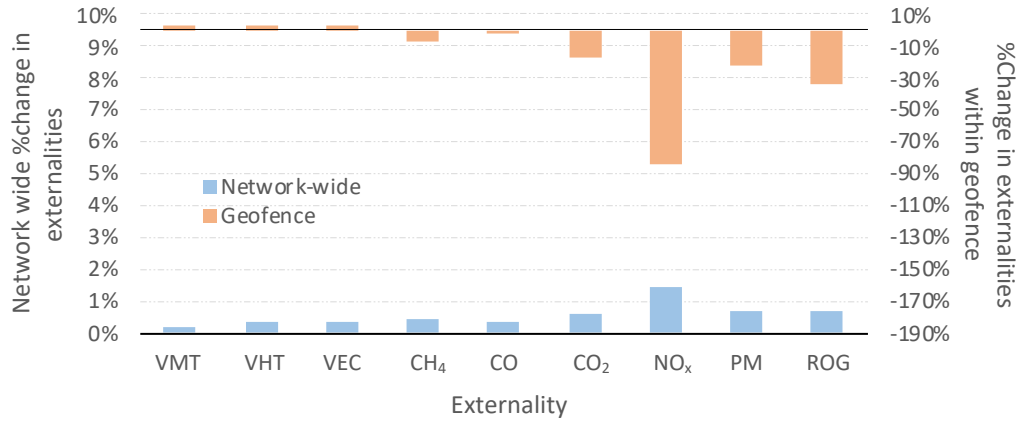


c) LCP assignment- with vs. without geofence

**Figure 15. Spatial effects of geofencing high CES score census tracts**

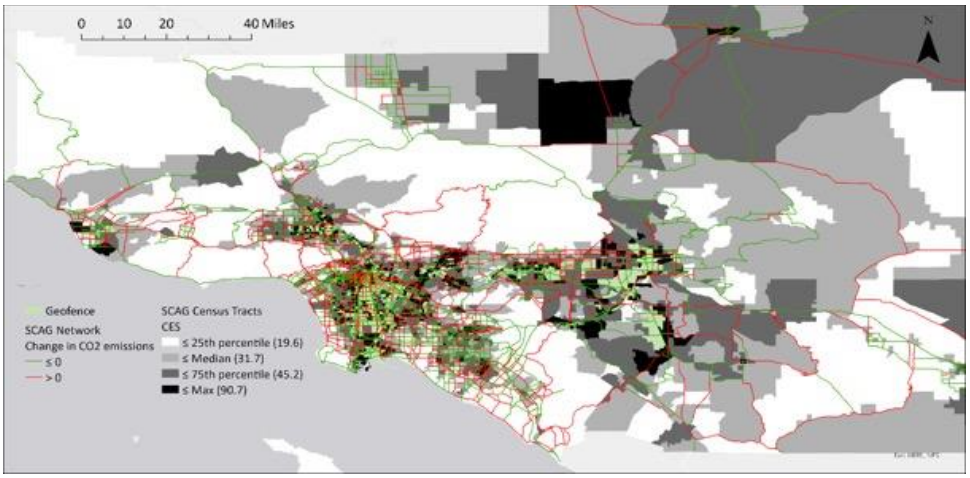


a) SP assignment- with vs. without geofence – Change in $CO_2$ emissions

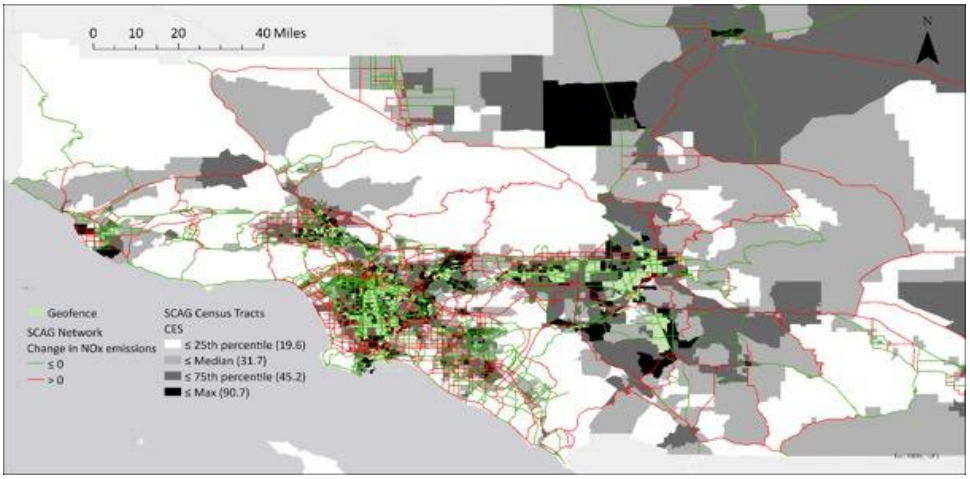


b) FP assignment- with vs. without geofence – Change in $NO_x$ emissions

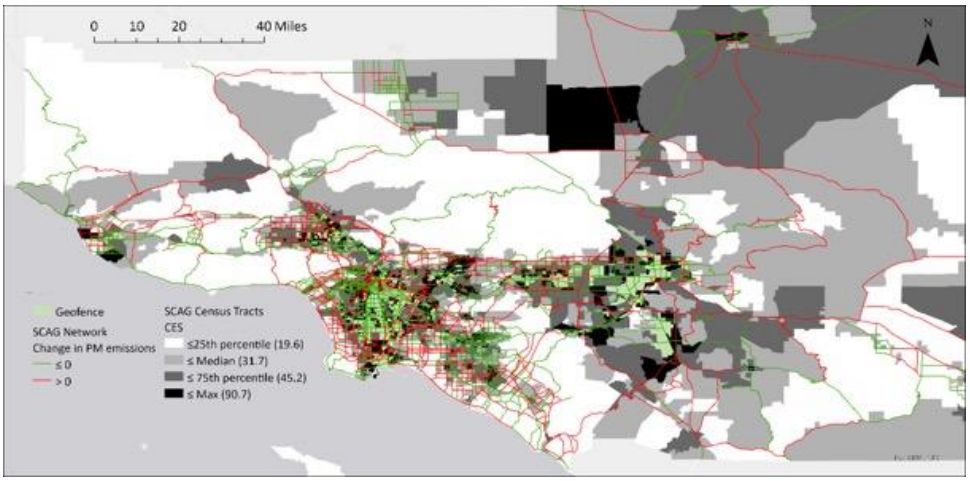


c) LCP assignment- with vs. without geofence – Change in PM emissions

# VI. Discussion

Can eco-routing be an important step towards sustainable zero-emission transportation? What are the costs and benefits of eco-routing for the stakeholders, i.e., the carrier and the system? This study is an effort to explore these lines of inquiry. The authors found an obvious trade-off or counterbalance between increased carrier costs and reductions in emissions from eco-routing, highlighting the lack of incentive for carriers to choose to eco-route. This result shouldn't be surprising; had there been a monetary advantage for carriers to reduce emissions, carriers would be eco-routing consistently. Yet, what is interesting are the cost-benefit analyses of eco-routing for the whole system, the carrier and society put together. This work found a net monetary loss for the system from eco-routing, as the monetary gain in the form of reduced emissions for society were more than compensated for by a monetary loss in the form of increased costs of hauling for the carrier. Had the benefits from $NO_x$ and $CO_2$ reductions been at least 10 times more valuable to society, eco-routing could have provided a net gain for the system. While $NO_x$ and $CO_2$ are the two most viable eco-routes, on the other end of spectrum is $CH_4$, the benefits of which need to be 0.1 million times more valuable for methane eco-routing to be viable for the system. While the study's analyses present a less-than encouraging picture for eco-routing, it is possible that carriers might still want to eco-route. Despite an increase in cost for the carrier, other important travel metrics relevant to the carrier may reduce due to eco-routing. For instance, this study found a 5.2% reduction in fuel consumption and a 6.9% reduction in travel distance from carbon-dioxide eco-routing (3.5% reduction in $CO_2$) for a carrier otherwise routing its fleet for shortest path.

To further establish the potential of eco-routing, this study considered its network-wide effects by developing a multi-class improved Traffic Assignment by Paired Alternative Segments (m-iTAPAS) algorithm. For current congestion levels, the authors found very modest reductions in network-wide emissions from trucks eco-routing. This is largely due to 95% of the traffic being passenger cars. However, this study found reductions to peak at lower passenger car traffic concentrations, which is around 20% of the current demand level. This highlights the potential of eco-routing to reduce emissions during off-peak hours, i.e., early morning and late night, when passenger car traffic is significantly lower. Yet it is important to note that while emissions may reduce on aggregate, certain parts of the region may observe a significant rise in emissions. This is particularly important in the context of criteria pollutants such as $NO_x$ and PM, which can adversely affect human health. However, the authors also found that such spatial variations in the emissions did not disproportionately affect, either positively or negatively, the disadvantaged communities in the SCAG region. Thus, certain disadvantaged communities observed an increase in emissions, while other disadvantaged communities in equal effect observed a reduction in emissions.

Given the lack of carrier incentive to eco-route, and the possibility of increased emissions for certain disadvantaged communities, this work explores geofencing as a tool to protect disadvantaged communities in the region. Today, disadvantaged communities in the area experience a disproportionate burden from freight activity. For this purpose, the authors

developed two geofences, one for the well-defined South East LA (SELA) region, thus exploring a real-life example of a disadvantaged community, and another with the high CalEnviroScreen (CES) score census tracts forming a non-contiguous and non-continuous region, thus exploring an extreme case of geofencing. In both of the cases, emissions within the geofence reduced significantly due to reduced truck travel, although the geofence area may experience increased passenger car traffic. Like with eco-routing, these reductions in emissions for the geofence area brings along increases in emissions elsewhere in the region. These impacts, as discussed, do not disproportionally affect other disadvantaged communities in the region. Thus, geofencing can bring about a desired outcome in the form of reductions in emissions for the disadvantaged region, with minimal but equitable increase in network-wide emissions.

The findings from this research will help support planning activities within the State, and contribute to the goals of having and efficient, sustainable, and competitive system. Results are relevant to policies such as Sustainable Communities, the Senate Bill 535 released by the Office of Environmental Health Hazard Assessment (OEHHA), the Climate Protection Act of 2008 (SB 375), and the California Global Warming Solutions Act of 2006 (AB 32). More importantly, the findings could help inform agency activities related to the implementation of strategies and efforts as part of the Community Air Protection Program, developed in response to Assembly Bill 617. Additionally, although the focus of the work was not to address zero emission vehicle technologies, the models will be updated and these technologies considered in future work.

# VII. References

AAA Gas Prices, n.d. AAA Gas Prices.

Ahn, K., Rakha, H., 2008. The effects of route choice decisions on vehicle energy consumption and emissions. *Transportation Research Part D: Transport and Environment* 13(3), 151-167.

Aziz, H.M.A., Ukkusuri, S.V., 2014. Exploring the trade-off between greenhouse gas emissions and travel time in daily travel decisions: Route and departure time choices. *Transportation Research Part D: Transport and Environment* 32, 334-353.

Bandeira, J.M., Fontes, T., Pereira, S.R., Fernandes, P., Khattak, A., Coelho, M.C., 2014. Assessing the Importance of Vehicle Type for the Implementation of Eco-routing Systems. *Transportation Research Procedia* 3, 800-809.

Bar-Gera, H., 2002. Origin-Based Algorithm for the Traffic Assignment Problem. *Transportation Science* 36(4), 398-417.

Bar-Gera, H., 2010. Traffic assignment by paired alternative segments. *Transportation Research Part B: Methodological* 44(8-9), 1022-1046.

Barth, M., Boriboonsomsin, K., 2008. Real-world carbon dioxide impacts of traffic congestion. *Transportation Research Record* 2058(1), 163-171.

Barth, M., Boriboonsomsin, K., 2009. Energy and emissions impacts of a freeway-based dynamic eco-driving system. *Transportation Research Part D: Transport and Environment* 14(6), 400-410.

Benedek, C.M., Rilett, L.R., 1998. Equitable traffic assignment with environmental cost functions. *Journal of Transportation Engineering* 124(1), 16-22.

Bezanson, J., Edelman, A., Karpinski, S., Shah, V.B., 2017. Julia: A fresh approach to numerical computing. *SIAM review* 59(1), 65-98.

Boriboonsomsin, K., Barth, M.J., Zhu, W., Vu, A., 2012. Eco-routing navigation system based on multisource historical and real-time traffic information. *IEEE Transactions on Intelligent Transportation Systems* 13(4), 1694-1704.

California Air Resources Board (CARB), 2017. EMFAC 2017 version 1.03.

California Environmental Protection Agency, n.d. Environmental Justice Program.

California Office of Environmental Health Hazard Assessment, 2017. CalEnviroScreen 3.0.

Caltrans, 2017. California Life-Cycle Benefit/Cost Analysis Model (Cal-B/C).

Dial, R.B., 2006. A path-based user-equilibrium traffic assignment algorithm that obviates path storage and enumeration. *Transportation Research Part B: Methodological* 40(10), 917-936.

Dijkstra, E.W., 1959. A note on two problems in connexion with graphs. *Numerische mathematik* 1(1), 269-271.

Elbery, A., Rakha, H., 2019. City-Wide Eco-Routing Navigation Considering Vehicular Communication Impacts. *Sensors (Basel)* 19(2).

Elbery, A., Rakha, H., ElNainay, M.Y., Drira, W., Filali, F., 2016. Eco-routing: Ant Colony based approach. *Proceedings of the International Conference on Vehicle Technology and Intelligent Transport Systems*, 31-38.

Environmental Protection Agency (EPA), 2019a. Sources of Greenhouse Gas Emissions.

Environmental Protection Agency (EPA), 2019b. State $CO_2$ Emissions from Fossil Fuel Combustion.

Environmental Protection Agency (EPA), 2020. Inventory of US Greenhouse Gas Emissions and Sinks: 1990 - 2018.

Erdoğan, S., Miller-Hooks, E., 2012. A green vehicle routing problem. *Transportation research part E: logistics and transportation review* 48(1), 100-114.

Ericsson, E., Larsson, H., Brundell-Freij, K., 2006. Optimizing route choice for lowest fuel consumption – Potential effects of a new driver support tool. *Transportation Research Part C: Emerging Technologies* 14(6), 369-383.

Figliozzi, M., 2010. Vehicle routing problem for emissions minimization. *Transportation Research Record* 2197(1), 1-7.

Guo, L., Huang, S., Sadek, A.W., 2012. An Evaluation of Environmental Benefits of Time-Dependent Green Routing in the Greater Buffalo–Niagara Region. *Journal of Intelligent Transportation Systems* 17(1), 18-30.

HERE Technologies, 2019. Traffic Flow Data - Traffic API.

Hooshmand, F., MirHassani, S., 2019. Time dependent green VRP with alternative fuel powered vehicles. *Energy Systems* 10(3), 721-756.

Huang, X., Peng, H., 2018. Eco-routing based on data driven fuel consumption model, In: University of Michigan, A.A. (Ed.).

Huang, Y., Ng, E.C.Y., Zhou, J.L., Surawski, N.C., Chan, E.F.C., Hong, G., 2018. Eco-driving technology for sustainable road transport: A review. *Renewable and Sustainable Energy Reviews* 93, 596-609.

Jaller, M., Pahwa, A., 2020. Evaluating the environmental impacts of online shopping: A behavioral and transportation approach. *Transportation Research Part D: Transport and Environment* 80.

Jaller, M., Pineda, L., 2017. Warehousing and Distribution Center Facilities in Southern California: The Use of the Commodity Flow Survey Data to Identify Logistics Sprawl and Freight Generation Patterns.

Jaller, M., Qian, X., Zhang, X., 2020a. E-commerce, Warehousing and Distribution Facilities in California: A Dynamic Landscape and the Impacts on Disadvantaged Communities.

Jaller, M., Rivera, D., Harvey, J., Kim, C., Lea, J., 2020b. Spatio-Temporal Analysis of Freight Patterns in Southern California.

Nagurney, A., 2000. Congested urban network and emissions paradox. *Transportation Research Part D: Transport and Environment* 5, 145-151.

Nagurney, A., Ramanujam, P., Dhanda, K.K., 1998. A multimodal traffic network equilibrium model with emission pollutant permits: compliance vs. non-compliance. *Transportation Research Part D: Transport and Environment* 3(5), 349-374.

Nie, Y., Li, Q., 2013. An eco-routing model considering microscopic vehicle operating conditions. *Transportation Research Part B: Methodological* 55, 154-170.

Pahwa, A., 2021. Freight Eco-Routing, v1.0-beta ed. GitHub.

Rakha, H.A., Ahn, K., Moran, K., 2012. INTEGRATION Framework for Modeling Eco-routing Strategies: Logic and Preliminary Results. *International Journal of Transportation Science and Technology* 1(3), 259-274.

Rilett, L.R., Benedek, C.M., 1994. Traffic Assignment under environmental and equity objectives. *Transportation Research Record*(1443).

Schröder, M., Cabral, P., 2019. Eco-friendly 3D-Routing: A GIS based 3D-Routing-Model to estimate and reduce CO2-emissions of distribution transports. *Computers, Environment and Urban Systems* 73, 40-55.

Scora, G., Boriboonsomsin, K., Barth, M., 2015. Value of eco-friendly route choice for heavy-duty trucks. *Research in Transportation Economics* 52, 3-14.

Sivak, M., Schoettle, B., 2012. Eco-driving: Strategic, tactical, and operational decisions of the driver that influence vehicle fuel economy. *Transport Policy* 22, 96-99.

Southern California Association of Governments, 2016. SCAG regional travel demand model and 2012 model validation.

Sugawara, S., Niemeier, D.A., 2000. How Much Can Vehicle Emissions be Reduced? *Transportation Research Record* 1815.

Sun, J., Liu, H.X., 2015. Stochastic Eco-routing in a Signalized Traffic Network. *Transportation Research Procedia* 7, 110-128.

Tiseo, I., 2020. World carbon dioxide emissions in 2018, by sector. Statista.

Tzeng, G.-H., Chen, C.-H., 1993. Multi-objective decision making for Traffic Assignment. *IEEE Transactions on Engineering Management* 40(2).

US Census Bureau, n.d. Census.

Weart, S.R., 2008. *The Discovery of Global Warming*. Harvard University Press.

Xie, J., Xie, C., 2016. New insights and improvements of using paired alternative segments for traffic assignment. *Transportation Research Part B: Methodological* 93, 406-424.

Yao, E., Song, Y., 2013. Study on Eco-Route Planning Algorithm and Environmental Impact Assessment. *Journal of Intelligent Transportation Systems* 17(1), 42-53.

Zeng, W., Miwa, T., Morikawa, T., 2016. Prediction of vehicle CO2 emission and its application to eco-routing navigation. *Transportation Research Part C: Emerging Technologies* 68, 194-214.

Zhou, M., Jin, H., Wang, W., 2016. A review of vehicle fuel consumption models to evaluate eco-driving and eco-routing. *Transportation Research Part D: Transport and Environment* 49, 203-218.

# VIII. Data Management

## Products of Research

This study develops two analytical tools using the Julia Programming Language -

1. Point-to-Point Routing tool (PPR) to evaluate private impacts of eco-routing for a carrier hauling diesel trucks in the Southern California Associating of Governments (SCAG) region.
2. Multi-class Traffic Assignment by Paired Alternative Segments (mTAPAS) to evaluate network-wide effects of system-wide freight eco-routing.

These two tools employ the SCAG regional network, and the CalEnviroScreen (CES) Scores for analyses. The Point-to-Point routing tool also employs HERE traffic API, a crowd-based platform to fetch vehicle speeds in the SCAG network. Additionally, the authors used the Air Resources Board' EMFAC model to estimate vehicle emission functions.

## Data Format and Content

The dataset contains SCAG network and origin-destination matrices, and CalEviroScreen scores in the .csv format. Additionally, the authors estimated speed functions for different types of network infrastructure using the data collected from HERE traffic.

## Data Access and Sharing

For SCAG files, the user is referred to https://scag.ca.gov/post/requesting-model-data to request the model data directly from SCAG.

Other SCAG related files can be accessed through SCAG GIS Open Data Portal https://gisdata-scag.opendata.arcgis.com/

Other files uploaded to Dryad are gathered from their public or open access systems and are provided as consolidated file sources to the research community and to replicate the findings of this research.

Interested individuals will be able to access the data available through Dryad and should contact the Principal Investigator, Dr. Miguel Jaller prior to accessing the data. The data should not be hosted in other locations and should only use the Dryad repository.

Users of the data should reference the system providers, and the data repository in Dryad. The DOI for the data is: https://doi.org/10.25338/B8934T

## Reuse and Redistribution

Dr. Miguel Jaller and the other co-authors of the work (identified in this Final Report) hold the intellectual property rights to the data and models generated by the research.

Data will not be able to be transferred to other data archives besides the ones approved by the PI and Co-PIs. The data can be used by anyone with proper referencing to the authors:

> Pahwa, Anmol; Jaller, Miguel (2021), Cargo routing and disadvantaged communities, Dryad, Dataset, https://doi.org/10.25338/B8934T

Other data is provided for reuse and redistribution under the MIT License.

# IX. Appendix

## Appendix A – Properties of the generalized cost function

To develop the necessary properties of the generalized cost function, authors further generalize and simplify the generalized cost function as a function on arc travel time, which itself is defined by the BPR function.

$$c_{ij} = \sum_{p\in P} \theta_p t_{ij} \sum_{k=0}^{2} \eta_k^p v_{ij}^k \tag{23}$$

$$c_{ij} = \left(Av_{ij}^2 + Bv_{ij} + C\right)t_{ij} \tag{24}$$

$$c_{ij} = \frac{Ad_{ij}^2}{t_{ij}} + B + Ct_{ij} \tag{25}$$

$$t_{ij} = t_{ij}^o\left(1 + \alpha_{ij}\left(\frac{x_{ij}}{V_{ij}}\right)^{\beta_{ij}}\right); t_{ij}^o, V_{ij} > 0;\ \alpha_{ij}, \beta_{ij} \geq 0 \tag{26}$$

The authors here assume $\left(Av_{ij}^2 + Bv_{ij} + C\right)$ to be strictly convex in $v_{ij}$, rendering $A > 0$. Such vehicle behavior is typical in context of vehicle efficiency, fuel consumption and emission rate. Now, in order to guarantee existence of the traffic assignment solution, uniqueness of the equilibrium and absence of infinite loops, this works assumes the generalized cost function to be continuously differentiable, monotonically non-decreasing and strictly positive, respectively, each of which are analyzed or imposed below.

1. Continuously differentiable

To establish continuous differentiability of $c_{ij}$, the analysis here establishes differentiability for $c_{ij}$ and continuity of $c'_{ij}$ in the domain of $c_{ij}$: $\mathbb{R}^+ \to \mathbb{R}$, where $\mathbb{R}^+$: $\{x_{ij} \in \mathbb{R}: x_{ij} \geq 0\}$.

$$c_{ij} = \frac{Ad_{ij}^2}{t_{ij}} + B + Ct_{ij} \tag{27}$$

$$c'_{ij} = \frac{dc_{ij}}{dx_{ij}} \tag{28}$$

$$c'_{ij} = \frac{t_{ij}^o \alpha_{ij}}{V_{ij}^{\beta_{ij}}}\left(C - \frac{Ad_{ij}^2}{t_{ij}^2}\right)x_{ij}^{\beta_{ij}-1} \tag{29}$$

Since $t_{ij} > 0$, $c_{ij}$ is continuous in its domain, while $c'_{ij}$ is continuous in the domain of $c_{ij}$ for $\beta_{ij} \geq 1$. Note, for $\beta_{ij} \in (0,1)$, $c'_{ij}$ is undefined at $x_{ij} = 0$, hence the condition, $\beta_{ij} \geq 1$ is essential for the generalized cost function to be continuously differentiable.

2. Monotonically non-decreasing

$$c'_{ij} \geq 0 \tag{30}$$

$$\frac{t_{ij}^{o}\alpha_{ij}}{v_{ij}^{\beta_{ij}}}\left(C - \frac{Ad_{ij}^{2}}{t_{ij}^{2}}\right)x_{ij}^{\beta_{ij}-1} \geq 0 \tag{31}$$

$$C - \frac{Ad_{ij}^{2}}{t_{ij}^{2}} \geq 0 \tag{32}$$

$$\frac{C}{A} \geq v_{ij}^{2} \tag{33}$$

The above condition must hold true for the maximum possible speed in the network, thus,

$$\frac{C}{A} \geq \max_{(i,j) \in A} {v_{ij}^{o}}^{2} \tag{34}$$

3. Strictly positive

Since the generalized cost function is monotonically non-decreasing, $c_{ij} > 0$ at $x_{ij} = 0$ ensures strict positivity, thus,

$$\frac{Ad_{ij}^{2}}{t_{ij}^{o}} + B + Ct_{ij}^{o} > 0 \tag{35}$$

$$B > -\left(\frac{Ad_{ij}^{2}}{t_{ij}^{o}} + Ct_{ij}^{o}\right) \tag{36}$$

For above condition to hold true for all arcs,

$$B > \max_{(i,j) \in A} -\left(\frac{Ad_{ij}^{2}}{t_{ij}^{o}} + Ct_{ij}^{o}\right) \tag{37}$$

$$B > \min_{(i,j) \in A} \left(\frac{Ad_{ij}^{2}}{t_{ij}^{o}} + Ct_{ij}^{o}\right) \tag{38}$$

## Appendix B – Comparison of truck emissions between POLA and aggregated rates

**Figure 16. Emission rates for aggregated and POLA Heavy-Heavy Duty Truck (T7)**

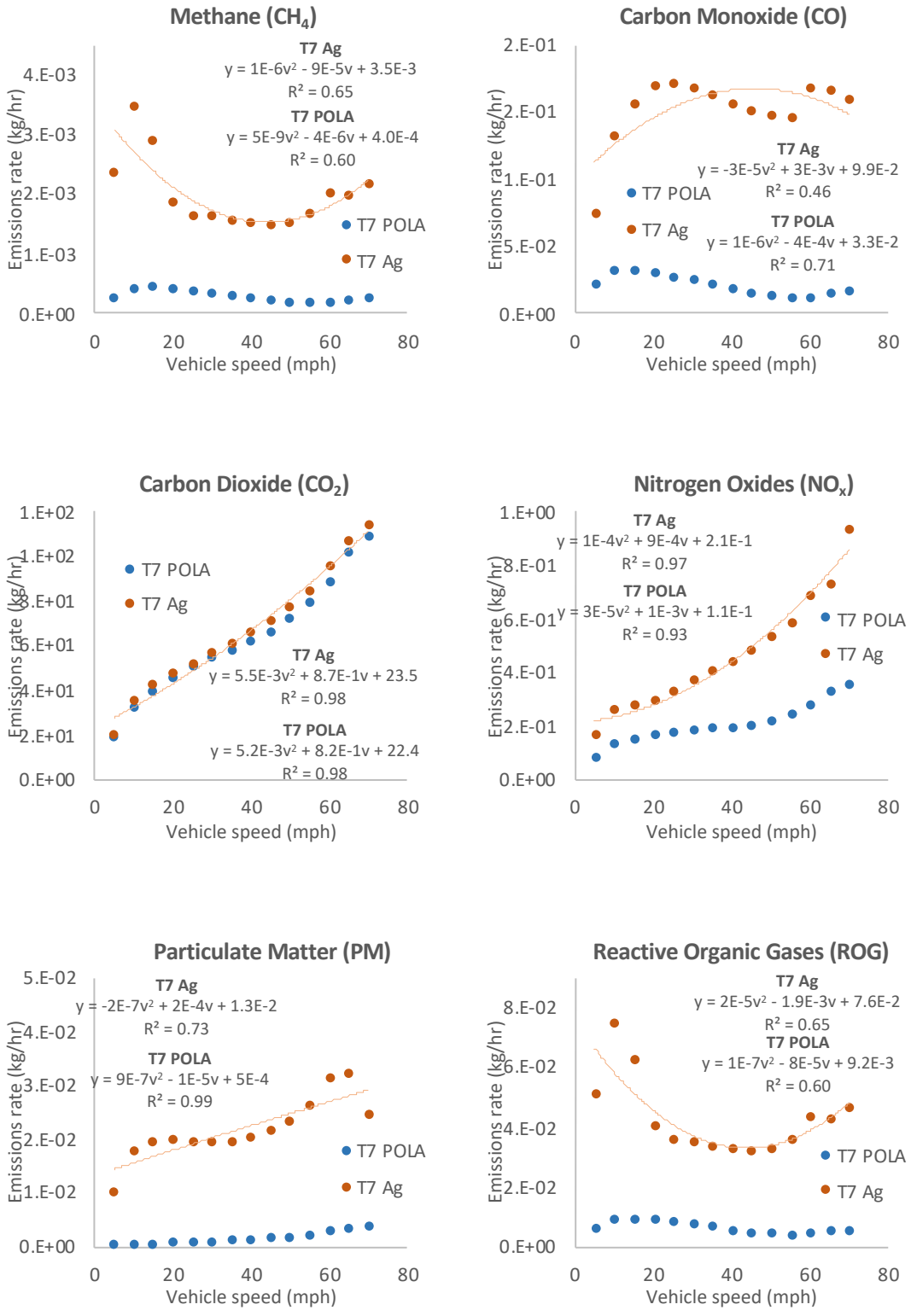

## Appendix C – Impact of eco-routing on HDT and LDA VMT

**Figure 17. Changes in VMT for trucks and passenger cars under eco-routing**

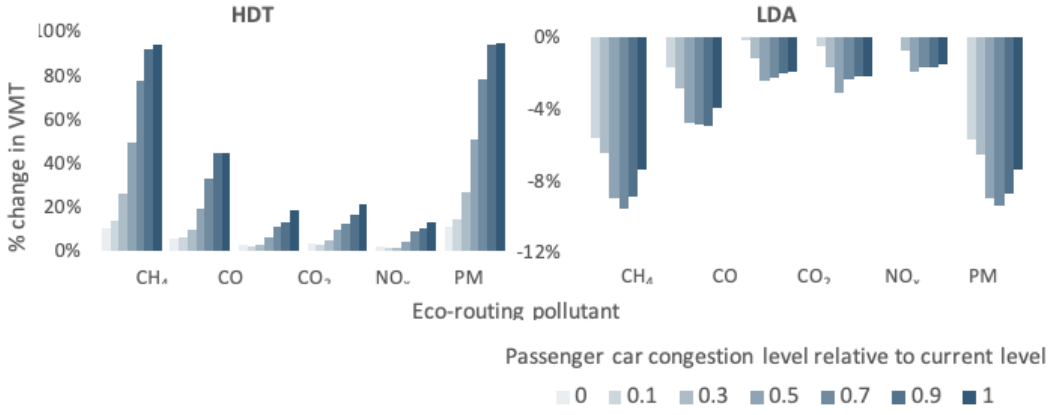


a) LEP assignment vs. SP assignment

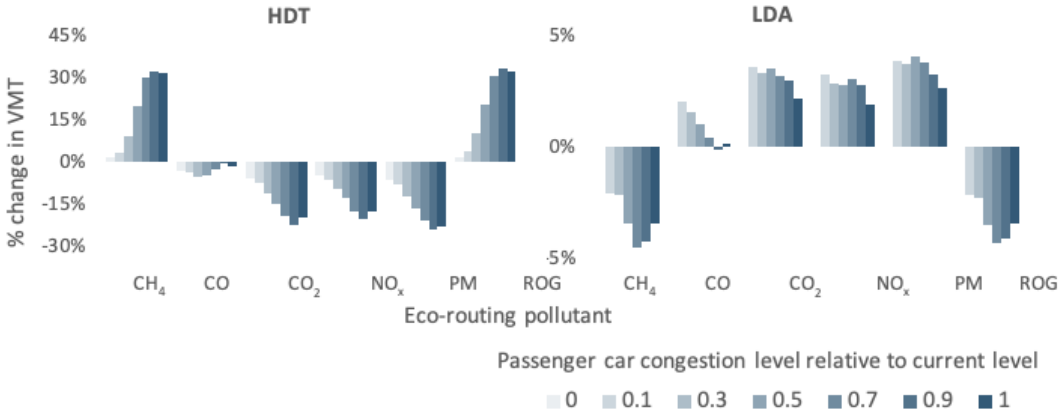


b) LEP assignment vs. FP assignment

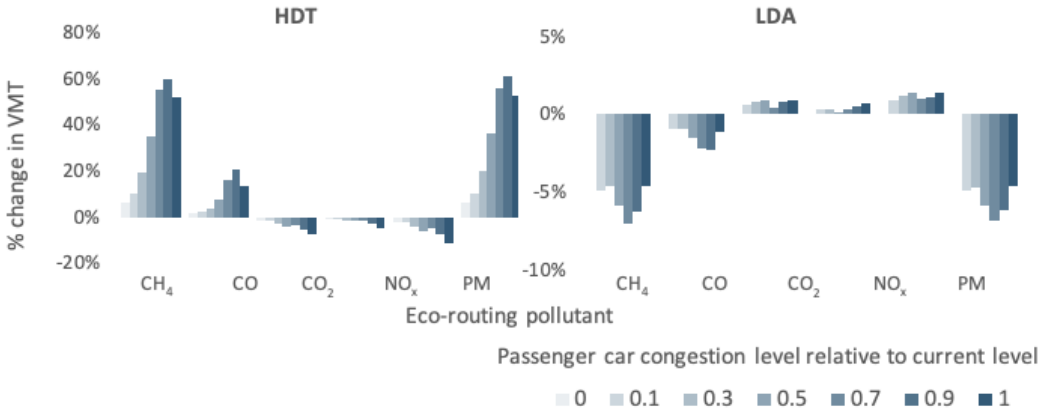


c) LEP assignment vs. LCP assignment